FEASIBILITY OF CONCENTRATED SOLAR THERMAL POWER PLANT FOR GRID CONNECTED SYSTEM IN SRI LANKA

G.A.S. Perera

(148361G)

Dissertation submitted in partial fulfillment of the requirements for the degree Master of Engineering

Department of Mechanical Engineering

University of Moratuwa

Sri Lanka

May 2019

DECLARATION

I declare that this is my own work and this dissertation does not incorporate without acknowledgement any material previously submitted for a degree or diploma in any other university or institute of higher learning and to the best of my knowledge and belief it does not contain any material previously published or written by another person except where the acknowledgement is made in the text.

Also, I hereby grant to University of Moratuwa the non-exclusive right to reproduce and distribute my dissertation, in whole or in part in print, electronic or other medium. I retain the right to use this content in whole or part in future works (such as articles or books).

---------- ----------

(Signature) (Date)

The above candidate has carried out research for the Masters dissertation under my supervision.

---------- ----------

(Signature of the supervisor) (Date)

Abstract

Electricity generation through concentrated solar thermal energy is a rapid developing technology in the world. In order to successfully adapt this technology for Sri Lankan conditions, it is necessary to identify the suitable technology and suitable locations in the country. Also it is a must to evaluate how a small scale concentrated solar power plant performs as the first step since it is a new technology for the country. This research focused on selecting the most suitable technology and location for implementing a concentrated solar power plant through literature review and studying how it performs technically and financially through a software simulation.

Literature review depicted that the parabolic trough is the most suitable technology since it is commercially well proven and most matured technology for grid connected power generation systems. Hambanthota is most suitable location in the country since its Direct Normal Irradiation level is more than 1600 kWh/m^2/year. An empherical model of a parabolic trough solar thermal plant of capacity 10 MWe at Hambanthota was simulated using the software, System Advisor Model to obtain the performance parameters. This study further focused on finding out the optimum value of solar multiple, the optimum size of thermal energy storage, the best heat transfer fluid and best collector type for the plant under study.

Simulation results has shown that a 10 MWe plant can generate 45.8 GWh in the first year with a capacity factor 52.8%. Optimum solar multiple was 3.5 while the optimum thermal energy storage size was 7 hours. Therminol 66 was identified as the most suitable heat transfer fluid and Solargenix SGX-1 was the suitable collector type for this application. The levelized cost of energy was 0.276 $/kWh which is a high value at the moment. The internal rate of return was 3.6% and the net present value was negative indicating that the project is not financially attractive for the investors. The power purchasing agreement price for solar PV, which is 0.1148 $/kWh was used in this simulation. This study was further extended to see how the plant financially performs in future, considering the rate of capital cost reduction of 30% for solar thermal plants in future for every five years time. It has been identified that the project is financially feasible to start after 15 years resulting a positive net present value and levelized cost of energy 0.11 $/kWh. A comparative analysis has shown that it takes more than 15 years for a plant without storage to be financially feasible. Future work is needed to validate the results of the simulation by a physical model.

Key words – Concentrated solar power, Parabolic trough, Direct Normal Irradiation, System Advisor Model, Solar multiple, Heat transfer fluid, Thermal energy storage, Levelized cost of Energy, Net present value

ACKNOWLEDGEMENTS

I take this opportunity to acknowledge all individuals and organizations that supported me in carrying out this research and writing the thesis from the beginning to the end.

First of all I should thank Professor R. A. Attalage, former Deputy Vice Chancellor, Senior Professor in the Department of Mechanical Engineering, University of Moratuwa for his guidance and comments given as the supervisor of this research.

Special thank goes to Dr. I. Mahakalanda, Director of undergraduate studies, Faculty of Business, Head of the Department of Industrial Management, University of Moratuwa for his valuable support given to me in completion of this research.

My heartiest gratitude is delivered to Dr. H.K.G. Punchihewa, Senior Lecturer, Department of Mechanical Engineering, Faculty of Engineering, University of Moratuwa for his incomparable contribution and encouragement given me by arranging progress review sessions and adding valuable comments and also for his hard work as the course coordinator.

I should thank Dr. R.A.C.P. Ranasinghe, Dr. M.M.I.D. Manthilaka and Dr. M.A. Wijewardhana, Senior Lecturers of Department of Mechanical Engineering, Faculty of Engineering, University of Moratuwa for their valuable comments during the progress review sessions of this research.

I would like to thank Mr. S.D.L. Sandanayake for his support given to me from the start to the end of the course.

Finally I herewith acknowledge Dr. Hilary E. Silva, former Director General, Sri Lanka Institute of Advanced Technological Education, Mr. P.G.L.S. Kumara, Acting Director, Advanced Technological Institute, Colombo and all the academic staff members of Advanced Technological Institute, Colombo for giving me support and encouragement to make this study a success.

TABLE OF CONTENTS

Declaration of the candidate and supervisor i

Abstract ii

Acknowledgements iii

Table of Contents iv

List of Figures vii

List of Tables x

List of Abbreviations xi

List of Appendices xiii

1 Introduction 1

2 Literature Review 4

2.1 Concentrated solar thermal plant 4

2.2 Concentrating collector technologies 7

2.2.1 Parabolic trough collector 7

2.2.2 Heliostat field collector 10

2.2.3 Linear Fresnel reflector 12

2.2.4 Parabolic dish collector 14

2.2.5 Solar chimney plant 16

2.3 Comparison of CSP technologies 17

2.4 Thermal Energy storage 21

2.5 Backup systems 23

2.6 Heat Transfer Fluids 24

2.7 Future cost of CSP plants 25

2.8 Simulation software tools for CSP plants 27

2.9 Solar Irradiation of Sri Lanka 28

3 Theory 31

3.1 Concentration Ratio 31

3.2 Useful Energy Collected 32

3.3 Levelized Cost of Energy 33

4 Methodology 35

4.1 Location and Resource 35

4.2 Solar Field 37

4.2.1 Solar Multiple 37

4.2.2 Heat Transfer Fluid 38

4.3 Solar Collector Assembly 38

4.4 Heat Collection Element 40

4.5 Power Block 40

4.6 Thermal Storage 42

4.6.1 Thermal Energy Storage 42

4.6.2 TES dispatch control 43

4.7 Parasitic Energy 44

4.8 System Costs 44

4.9 System Performance Degradation 45

4.10 Financial Parameters 45

4.11 PPA price for positive NPV 46

4.12 Future cost of proposed CSP plant 46

4.13 Sensitivity analysis for discount rate 48

4.14 Performance analysis for uncertainty of DNI data 48

4.15 Performance of 25 MWe and 50 MWe plants 48

5 Results 49

5.1 Solar Multiple and Thermal Energy Storage 49

5.2 Heat Transfer Fluid 50

5.3 Selection of SCA 53

5.4 Performance of 10 MWe plant 54

5.4.1 Technical Performance 54

5.4.2 Financial Performance 55

5.5 Energy profiles of 10 MWe plant 58

5.6 PPA price for positive NPV 60

5.7 Results for DNI data uncertanity 61

5.8 Project feasibility analysis for future cost 62

5.8 Sensitivity analysis for discount rate 70

5.9 Performance of 25 MWe and 50 MWe plants 72

6 Discussion 73

7 Conclusion 77

References 78

List of Figures

Figure 2.1: Main parts of CSP plant and their components 4

Figure 2.2: Steam power plant operates on Rankine cycle 5

Figure 2.3: Direct and diffuse solar radiation 6

Figure 2.4: Technologywise installation of CSP plants in the world 6

Figure 2.5: Schematic of parabolic trough collector 8

Figure 2.6: Rim angle and focal line of parabolic trough 8

Figure 2.7: The receiver or HCE of parabolic trough collector 9

Figure 2.8: Schematic of heliostat field collector 11

Figure 2.9: Volumetric air receiver 12

Figure 2.10: Schematic of LFR design 13

Figure 2.11: The design of CLFR system 14

Figure 2.12: Secondary reflector of CLFR 14

Figure 2.13: Schematic of parabolic dish collector 15

Figure 2.14: The cavity receiver of PDC plant 15

Figure 2.15: Solar chimney principle 17

Figure 2.16: CSP plant with thermal energy storage 22

Figure 2.17: Performance of CSP plant with TES and back up (a) and sloe TES(b) 23

Figure 2.18: LCOE and auction price trend for CSP, 2010 - 2022 24

Figure 2.19: Direct normal solar irradiation map of Sri Lanka 29

Figure 3.1: Relation between receiver temperature and concentration ratio 32

Figure 4.1: Hourly variation of DNI and temperature 36

Figure 5.1: Variation of LCOE with Solar Multiple and TES size 50

Figure 5.2: Annual energy output with HTF types 51

Figure 5.3: Capacity factor with THF types 51

Figure 5.4: LCOE with HTF types 52

Figure 5.5: IRR with HTF types 52

Figure 5.6: Annual energy output with SCA types 53

Figure 5.7: IRR with SCA types 53

Figure 5.8: LCOE w SCA types 54

Figure 5.9: Annual energy production with number of years 57

Figure 5.10: Monthly first year energy generation 57

Figure 5.11: Monthly and annual thermal power incident and absorbed 58

Figure 5.12: Monthly and annual TES performance 59

Figure 5.13: Monthly and annual electrical power output of the plant 60

Figure 5.14: Variation of LCOE with project starting time 63

Figure 5.15: Variation of IRR with project starting time 64

Figure 5.16: Variation of NPV with project starting time 64

Figure 5.17: LCOE vs Storage size at different starting times 66

Figure 5.18: IRR vs Storage size at different starting times 66

Figure 5.19: NPV vs Storage size at different starting times 67

Figure 5.20: LCOE with project starting time at different cost reduction rates (with 7 hrs storage) 68

Figure 5.21: NPV with project starting time at different cost reduction rates (with 7 hrs storage) 68

Figure 5.22: LCOE with project starting time at different cost reduction rates (without storage) 69

Figure 5.23: NPV with project starting time at different cost reduction rates (without storage) 69

Figure 5.24: NPV with project starting time at different discount rates (with 7 hrs storage) 70

Figure 5.25: LCOE with project starting time at different discount rates (with 7 hrs storage) 70

Figure 5.26: NPV with project starting time at different discount rates (without storage) 71

Figure 5.27: LCOE with project starting time at different discount rates (without storage) 71

List of Tables

Table 2.1: Technical performance data of CSP technologies 18

Table 2.2: Operating conditions of CSP technologies 19

Table 2.3: Financial performance of CSP technologies 20

Table 2.4: Environmental aspects and technology maturity 20

Table 2.5: Properties of commonly used HTFs 24

Table 2.6: DNI data of Sri Lanka 30

Table 4.1: Location and annual weather data summary for Hambanthota 37

Table 4.2: Major properties of available SCA types in SAM library 39

Table 4.3: Reference system turbine details in SAM library 41

Table 4.4: Library data of parasitic electric energy use 44

Table 4.5: Direct capital costs default values 45

Table 5.1: Simulation results for selecting TES size and Solar Multiple 49

Table 5.2: Results from the solar field page 55

Table 5.3: Direct capital costs for 10 MWe plant 55

Table 5.4: Indirect costs of the plant 56

Table 5.5: Summary of results for 10 MWe plant 56

Table 5.6: Increase in NPV with PPA price 61

Table 5.7: Plant performance at ± 5% DNI 62

Table 5.8: Comparison of 25 MWe and 50 MWe plants with 10 MWe plant 72

List of Abbreviations

Abbreviation	Description
CLFR	Compact Linear Fresnel Reflector
CSP	Concentrated Solar Power
CWEC	Canadian Weather for Energy Calculation
DNI	Direct Normal Irradiation
DSG	Direct Steam Generation
HCE	Heat Collection Element
HFC	Heliostat Field Collector
HTF	Heat Transfer Fluid
IRENA	International Renewable Energy Agency
IRR	Internal Rate of Return
ISCC	Integrated Solar Combined Cycle
IWEC	International Weather for Energy Calculation
LCOE	Levelized Cost of Energy
LFR	Linear Fresnel Reflector
NPV	Net Present Value
NREL	National Renewable Energy Laboratory
NSRDB	National Solar Resource Data Base
PDC	Parabolic Dish Collector
PPA	Power Purchase Agreement

PTC	Parabolic Trough Collector
PV	Photovoltaics
SAM	System Advisor Model
SCA	Solar Collector Assembly
SM	Solar Multiple
SWERA	Solar Wind Energy Resource Assessment
TES	Thermal Energy Storage

List of Appendices

Appendix	Description	Page
Appendix A	Location and Resource page (SAM)	83
Appendix B	Solar field page (SAM)	84
Appendix C	Solar Collector Assembly page (SAM)	84
Appendix D	Heat Collection Element page (SAM)	85
Appendix E	Power Block page (SAM)	86
Appendix F	Thermal Energy Storage page (SAM)	87
Appendix G	System costs page (SAM)	88
Appendix H	Financial parameters page (SAM)	89

1 INTRODUCTION

The demand for energy is increasing day by day with the development of world economy and the increasing population. To cater this energy requirement fossil fuel is used as the main source since it is widely available at low cost and easy to convert in to useful energy forms. However it is noticed that due to high rate of consumption fossil fuel sources are depleting rapidly. Burning of fossil fuel causes so many environmental problems such as acid rains, ozone layer depletion and climate changes. As a result, more research and developments were done on renewable energy sector during past two decades. Solar energy, wind energy, bio-mass energy, tidal energy and geothermal energy are the main sources of renewable energy.

Among these renewable energy sources, solar energy is the most vital source as it is freely available, non-depleting nature and cleanliness. Economic growth, environmental protection, diversity of fuel supply and rapid deployment are some of the benefits of adopting to solar energy [1]. Creation of jobs and potential for technology transfer and innovation are also some advantages of it [1]. Solar energy can be used to generate electricity, space heating, industrial process heating, refrigeration, gas reforming and metal production. Among them, electricity generation is a successful and commercially proven application over the past two decades. Two technologies used to produce electrical power from solar energy are photovoltaics (PV) and concentrated solar power (CSP). Photovoltaics generate electricity directly by the photovoltaic effect of materials. CSP captures thermal energy from solar radiation and convert it to mechanical energy and then generate electricity via generators. Power generation from CSP is still in its early stages and some of the plants are still in the demonstration level. By year 2016 the total installed capacity of CSP in power generation was only 4.8 GWe while the total installed capacity of solar PV is 303 GWe [2]. The top five countries of CSP technology based on the installed capacity are Spain, United States, India, South Africa and Morocco [2]. Spain and United States share over 80% of the solar thermal based power generation in the world. China, Australia and Middle East are among other countries who are using this technology to cater their energy needs. Since the CSP technology is still in its early stages the cost of energy is high compared to the other renewable energy technologies

at present. It is expected that the cost will decrease significantly due to the technology learning and competitiveness in future.

Sri Lanka also face the challenge of increasing needs of electricity from 70,000 GWh in year 2016 to 140,000 GWh in year 2050 [3]. The country is also planning to generate electricity through 100% renewable energy sources by year 2050. As a part of its energy sector development plan Sri Lanka aims to become energy self-sufficient by year 2030. In order to achieve above goals the country has to look at new options available in the power generation sector with renewable energy sources while developing the existing technologies. The country still primarily depend on fossil fuel in power generation and it was 52% by year 2015. At present hydro power, solar PV, wind energy and biomass plants are in operation for power generation in the country from renewable sources. In addition to that the country will have to look at its potential of generating electricity using concentrated solar thermal energy, geothermal energy and tidal energy in order to achieve the above mentioned goals.

When achieving the target of generating electricity using 100% renewable energy sources the country has to face a number of key challenges in technical and financial aspects. A large amount of investment is required in infrastructure development and non-availability of proper incentives to develop renewable energy based capacities are among them. Lack of local research and development to promote local capacity development is also an issue. At present the cost of electricity from renewable energy sources are comparatively high. With technological innovation it is expected that the price to be drop in renewable energy based electricity in future.

When using solar energy as a source of electricity generation, at present, the country is only looking at solar PV technology. No proper research has been conducted yet in order to find out the potential of electricity generation through CSP technology and its financial performance in the country. There are different technologies used to capture solar thermal energy for power generation at international level. Different technologies have different levels of technical performance, financial performance, operating conditions and maturity. One objective of this study is to select the most suitable CSP technology for the country by considering their current performance.

The level of solar radiation is different from location to location in the country. The study focuses on selecting the best location in the country for implementing a CSP plant. The potential of electricity generation by a suitable technology at a selected location in the country has to be analyzed. The next objective is to find out how a CSP plant performs technically and financially. In order to get the optimum performance of the plant, suitable values for the plant parameters need to be find out. When considering the future cost reduction of the CSP technologies, how the plant financially performs in future also has to be analyzed. Finding out the rates of cost reduction and analyzing the financial performance of the plant according to them is another objective of this research.

In the literature review the different CSP technologies used to capture and store solar thermal energy and the methods used to generate power in the world being studied. The performance indices and maturity level of these different CSP technologies were compared in the study. The literature review includes the solar resource assessment data of the country in order to find out suitable locations for implementing CSP. To find out how a concentrated solar thermal power plant performs in Sri Lanka, a software simulation was performed by identifying a suitable software. This study investigates the technical and financial performance of a 10 MWe parabolic trough concentrated solar thermal power plant at Hambanthota through the software simulation. System Advisor Model (SAM) which is provided by National Renewable Energy Laboratory (NREL) was used for this purpose. Parametric simulations were performed to find out a best value for solar multiple, optimum size of thermal energy storage, best type of solar collector assembly (SCA) and best type of heat transfer fluid (HTF). To check the financial feasibility of the plant under study, financial performance indices such as levelized cost of energy (LCOE), net present value (NPV) and internal rate of return (IRR) were calculated. Further the study has compared the performance of plants with capacities 25 MWe and 50 MWe at the same location. Since it was noticed that the CSP projects for the country is not financially attractive at present due to the high cost, the study was extended to see in which year it is going to be feasible in future based on the trend of capital cost reduction.

2 LITERATURE REVIEW

2.1 Concentrated solar thermal plant

Concentrating solar power is a proven renewable energy technology for electricity generation. It is a technology used to capture the energy received to earth through solar radiation and focuses it to a receiver with smaller area. CSP plant consists of three main parts as solar field, power block and thermal storage unit as shown in Figure 2.1.

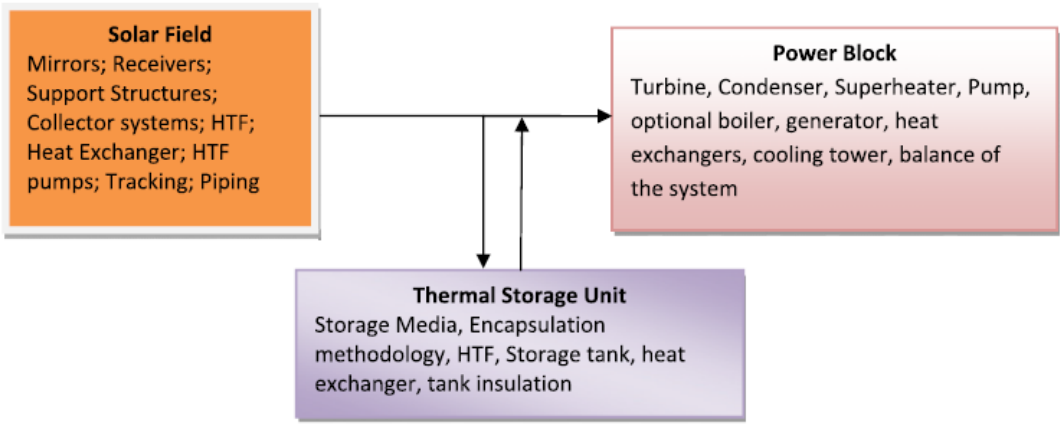

Figure 2.1: Main parts of a CSP plant and their components [4]

Mirrors in the solar field capture solar radiation and it is reflected to the receiver. The solar energy concentrated to the receiver is absorbed by the liquid that runs through it which is known as heat transfer fluid. It is usually synthetic oil, molten salt or water that collects energy at the receiver and transport it to the power generation block. While supplying heat to the power block the system interacts with a thermal energy storage in order to store part of the captured energy at peak hours of solar radiation. The storage supplies energy to the power block when the energy coming through direct line is not enough to run the turbine. Power generation block runs the Rankine cycle which is the basic thermodynamic cycle used to run a steam power plant. The basic Rankine cycle consists of a steam generator or boiler, steam turbine, condenser and pump as shown in Figure 2.2. Solar energy collected by the heat transfer fluid is transferred to water in a heat exchanger to generate steam to run the turbine. The steam

turbine is coupled with a generator which produces the electric power by converting mechanical energy in to electrical energy.

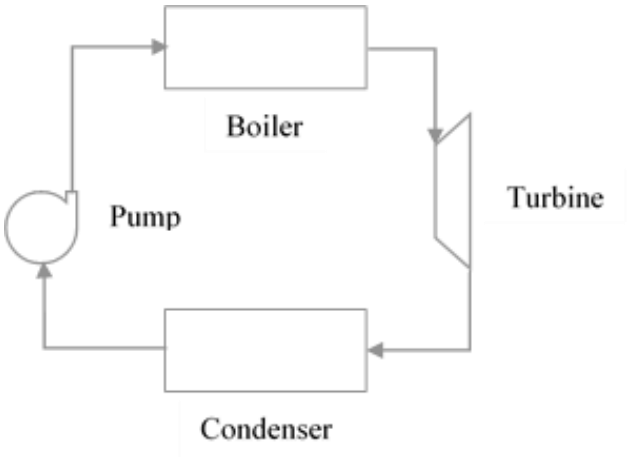

Figure 2.2: Simple steam power plant operates on Rankine cycle

Solar radiation received to the earth surface as direct and diffuse radiation. Direct component of solar radiation referred to as direct normal irradiance (DNI) or beam radiation is the component which is not scattered by the atmosphere. Solar radiation which is scattered by the atmosphere and which the direction has been changed referred to as diffuse radiation and it is illustrated in Figure 2.3. Unlike solar PV, CSP plants accept only the direct component of solar radiation for their operation. Therefore when locating CSP plants the locations with high DNI must be selected. Central and South America, South - Western United States, Mediterranean countries of Europe and South and North Africa are some of the most promising areas in the world for implementing CSP plants. Middle East, desert areas of India, Pakistan, Iran, Australia and China are also among them [1]. One square kilometre of land is enough to generate 100 – 120 GWh of electricity per year by concentrated solar thermal plants in many of these regions [1].

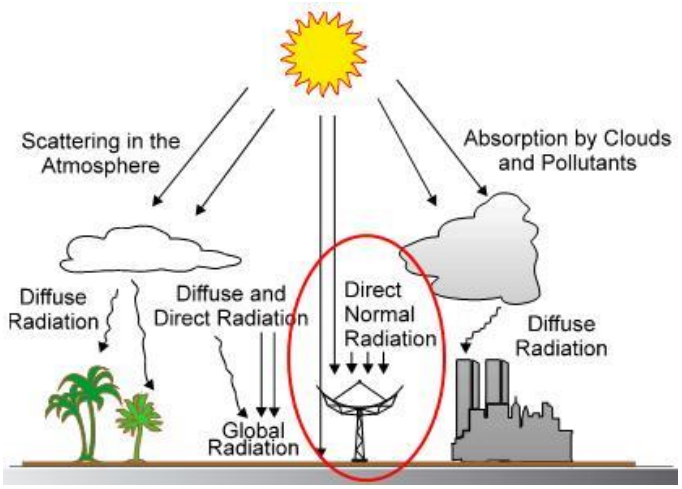

Figure 2.3: Direct and diffuse solar radiation [30]

Parabolic trough collector (PTC), heliostat field collector (HFC) or solar tower, linear Fresnel reflector (LFR) and parabolic dish collector (PDC) are the four main CSP technologies used in the world at present. Solar chimney technology is also another method of generation power from solar energy. Among the available technologies, the parabolic trough collector is the widely used technology in the world and over 96% of CSP plants use that technology to collect solar thermal energy [5]. Figure 2.4 is an illustration of the technology wise operation of CSP plants with their percentages.

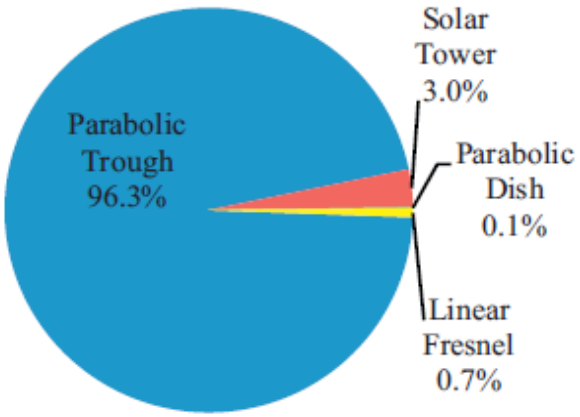

Figure 2.4: Technology wise operation of CSP in the world [5]

CSP plants are currently installed from medium to large scale. Most of them are located in Spain and United States [5]. Countries like Iran, Germany, Australia, Italy, South Africa and China also successfully use this technology to generate electricity from solar energy. Morocco, India, Saudi Arabia are few of the countries started to implement CSP for power generation in recent past. Morocco has added the first phase of the world's largest solar thermal plant to the grid very recently. First phase of the project is of the capacity of 160 MWe out of the total capacity of 580 MWe.

Different technologies have different features and when selecting a suitable technology for a particular application those must be considered. Fast development of these technologies makes it difficult to select which technology is best suited for a given condition. The selection become further complicated since there are several factors to be considered under technical, financial and environmental aspects. When evaluating different technologies, each has their own advantages and disadvantages compared to each other. This has been studied in detail in this literature review.

2.2 Concentrating collector technologies

2.2.1 Parabolic trough collector

The parabolic trough collector technology uses relatively long reflectors of parabolic shape which concentrate the parallel solar rays in to its focal line as illustrated in Figure 2.5. Number of reflectors are aligned parallel to each other in a single plant. The reflector is made out of Aluminium or steel and the mirrors are 4mm to 5mm thick and a Ultra Violet stabilized mirror film is laminated on to the aluminium substrate provides the reflectance of 0.94 [6].

The accuracy of the parabolic profile and the optical error tolerance are key factors for parabolic trough reflectors to be efficient. Fabrication method and strength of the materials used are also among them [6]. The factors which governs the amount of heat collected by the trough are the rim angle and the length [6]. Figure 2.6 illustrates the geometry of a parabolic trough.

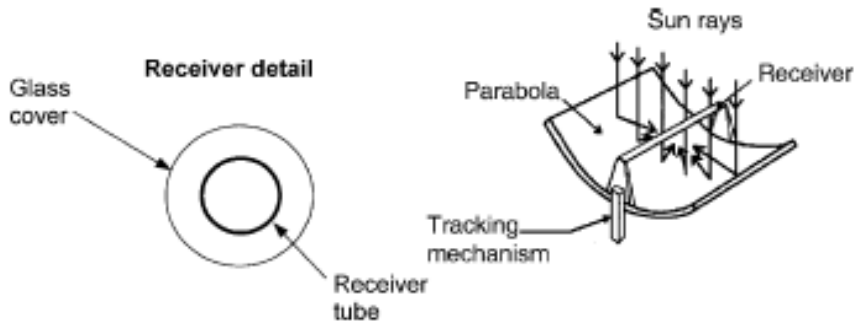

Figure 2.5: Schematic of parabolic trough collector [7]

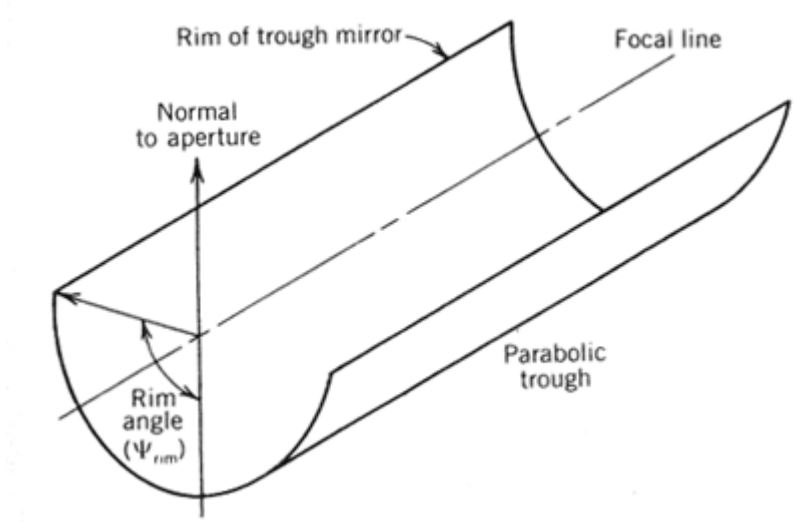

Figure 2.6: Rim angle and focal line of parabolic trough [31]

The parabolic troughs are mounted on steel or aluminium structures. Modern designs use structures made using aluminium space frame technology [6]. Single axis tracking mechanism is used in PTC units for focusing the collector towards the solar radiation during the day. In order to receive heat efficiently, the tracking mechanism should trace sun path very accurately. Since the collectors are often exposed to wind, the structure must be strong enough to withstand in wind loads and avoid the deflections for accurate focusing of the radiation to the receiver. Collectors are mounted in both north – south and east – west orientations. PTCs capture maximum amount of energy

from the sun annually when they are directed towards north – south orientation. However east – west orientation can capture more energy in summer months [7].

A long receiver pipe is placed at the focal line of the trough to collect the concentrated solar energy in order to heat the heat transfer fluid. High absorptance and low thermal losses are expected when designing the receiver. The level of shading also must be minimum [6]. The receiver consists of a stainless steel pipe which is coated by solar selective coating which has the absorptance over 0.95. This is enclosed in a glass tube which is vacuumed in order to reduce the convective heat losses. Figure 2.7 is an illustration of heat collection element (HCE) or the receiver.

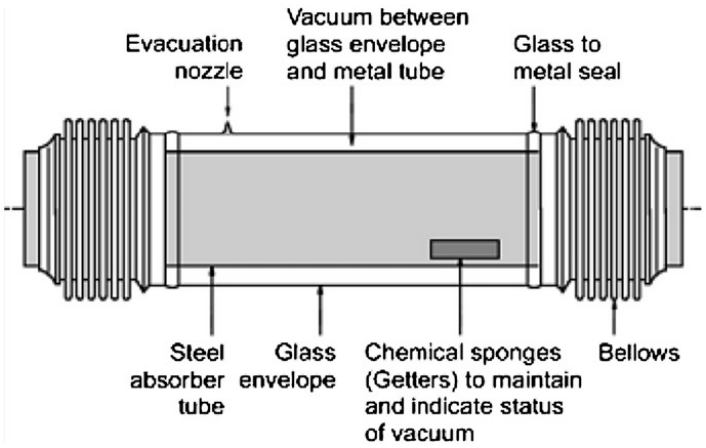

Figure 2.7: The receiver or HCE for parabolic trough collector [5]

Synthetic oil which is used as heat transfer medium is heated nearly to the temperature of 400^{o}C in the receiver [8]. Oil transfer heat through the collector pipes to the heat exchangers and the water is pre heated and then evaporated and superheated. The superheated steam is fed to turbine for power generation and returns to the condenser for cooling and again pumped to the heat exchangers. This completes the Rankine cycle which is the basic thermodynamic cycle used for power generation in steam power plants. Operating temperatures of the system is in the range of 20 ^{o}C to 400 ^{o}C [5] and the concentration ratio is 70 – 80 times [8]. The annual solar to electric conversion efficiency is around 15% [8]. Another technology used in the PTC plant is the generation of steam directly in the solar field known as direct steam generation (DSG). In these plants, heat transfer fluid is water, where water is boiled partially in

the receiver and circulated in a steam drum which separates steam from water. The recent innovations promotes the use of ionic fluids as heat transfer media. These ionic fluids are more heat resilient compared to oil. Therefore the possibility of corroding the receiver pipes is less [7]. But the use of ionic liquids in the system would increase the cost of operation.

Parabolic trough technology is the most advanced technology among the CSP technologies since there are lot of advances with considerable experience over the years. This is the most mature technology to generate temperatures up to 400 ^{o}C [9]. Largest PTC power plant in the world is the 354 MWe capacity plant in Mojawe desert, California.

2.2.2 Heliostat field collector

Heliostat field collector also referred as solar power tower utilizes a central receiver on a tower which is surrounded by an array of mirrors. Figure 2.8 is a sketch of the solar tower and HFCs. Solar rays fallen on to the mirrors are reflected to the central receiver. These heliostat mirrors are flat or slightly concave and mounted on pedestals. Each mirror is equipped with two axis tracking mechanism in order to direct solar radiation individually to the receiver throughout the day and during the year. These heliostats range from 50 to 150 m^2 in area [7]. Height of the solar towers used in these plant range from 75 to 150 m [7]. An advantage of this technology is thermal energy in the range of 200 to 1000 kW/m^2 can be focused in to the receiver. The solar flux reflected to the single receiver by number of mirrors yields very high concentration ratios of 1000 to 3000 suns [8]. Thus the HFC plants can operate at temperatures above 500 ^{o}C, providing high power conversion efficiency in the cycle.

Heat transfer fluid absorbs the heat collected at the central receiver and transfer to the water at heat exchanger to run the steam Rankine power cycle. DSG plants are also in operation at commercial level and some plants use molten salts to store and transfer heat.

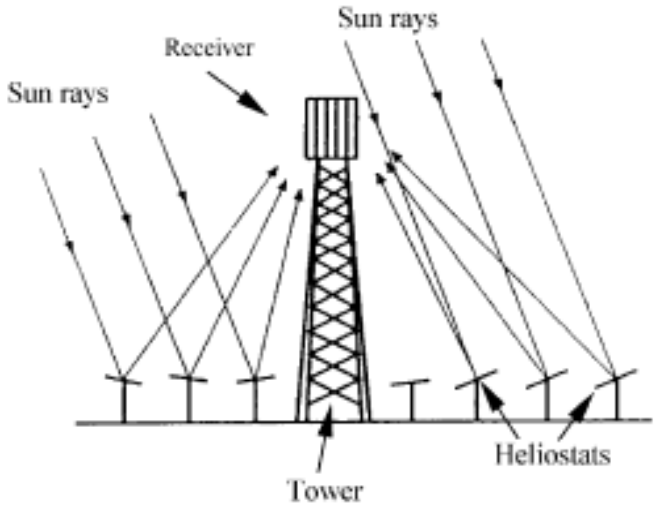

Figure 2.8: Schematic of heliostat field collector [7]

Compared to the other technologies the cost of HFC plants are high. Capital cost of these plants are around 3900 – 8300 $/kW [18] and operation and maintenance cost is 0.034 – 0.093 $/kW [10]. It is not economical to operate HFC plant in small scale. Large scale plants usually above 10 MWe are in operation today. Cost for the heliostats is nearly 50% of the total plant cost so that lot of efforts has been put on to reduce the cost by making them in larger size. Therefore the heliostat field cost has fallen to a level of 100 $/m^2 and the reduction of plant capital cost is expected to drop to a level of 2500 $/kW in future [10]. Because of the heliostat array the land requirement is comparatively high at around 8 – 12 m^2/MWh/year [8]. This technology mostly prefers level ground but hillsides also been used.

Solar powered gas turbine engines can also be used in the HFC technology since the operating temperatures are high due to high concentration ratios. For this purpose a volumetric air receiver has to be used to heat up air to the temperatures up to 1000 ^{o}C. Air is first compressed at the compressor and then heated at the receiver by solar energy. It is then send to the turbine for expansion to complete the Brayton cycle. The combined operation of Brayton and Rankine cycles are also possible which are known as integrated solar combined cycle (ISCC) plants. Figure 2.9 illustrates a volumetric air receiver.

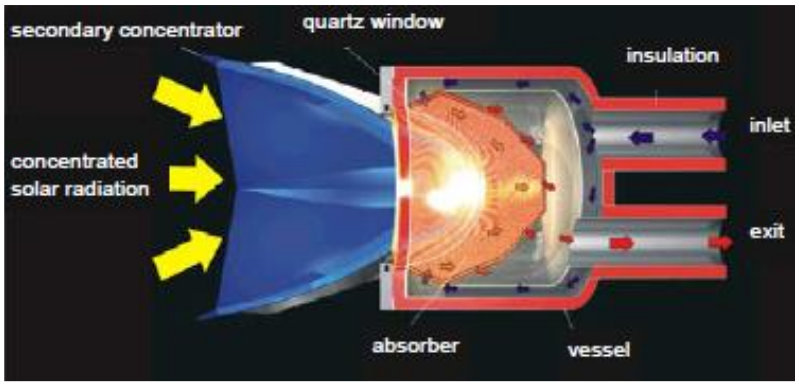

Figure 2.9: Schematic of volumetric air receiver [11]

Solar One and Solar Two are the first HFC plants with the capacity of 10 MWe, built in Mojave Desert, California. PS 10 and PS 20 HFC plants were recently completed in Spain [7]. Purpose of this project is to produce electricity in grid connected mode. In PS 10 plant which has the capacity of 11 MWe, the solar radiation is reflected to the receiver by 624 heliostats. Each heliostat unit has a reflective area of 121 m^2. The cavity receiver is a radiant boiler which can produce more than 100,000 kilograms of saturated steam at 40 bar and 250 ^oC in an hour [6]. The plant is also equipped with a thermal energy storage to have continuous operation at cloudy transient periods. PS 20 is 20 MWe plant has 1255 heliostat mirrors and the receiver is mounted on a tower of height 165 m [6]. Ivanpah solar power complex in California will be the world's largest power tower with the gross capacity of 392 MWe. Number of heliostats required for this is power complex is 173500. Boilers installed in the plant can generate superheated steam at 550 ^oC and 160 bar. Solar selective materials are used as coatings on the boiler tubes of the receiver in order to maximize energy absorptance. This power plant does not equipped with thermal energy storage.

2.2.3 Linear Fresnel reflector

Linear Fresnel reflectors are long arrays of flat mirrors which concentrate solar radiation on to a linear receiver tube above the mirrors. LFR uses similar principle in arrangement and operation to the PTC technology. The receiver is fixed on a tower which is 10 to 15 m in high from the ground level above the reflector field. The profile

of the structure is low and the mirrors are above 1 to 2 m from ground level. Therefore the plant can operate in strong winds and the structure could be simpler and light weight compared to PTC. Mirrors has single axis tracking mechanism to collect maximum radiation from the sun throughout the day as in the PTC. Since the technology uses flat mirrors which are easier to produce and cheaper, the cost of the reflector system is less compared to the other types. Also the manufacturers for this type of flat mirrors are available worldwide. Figure 2.10 is an illustration of the mirror and receiver arrangement of LFR plant.

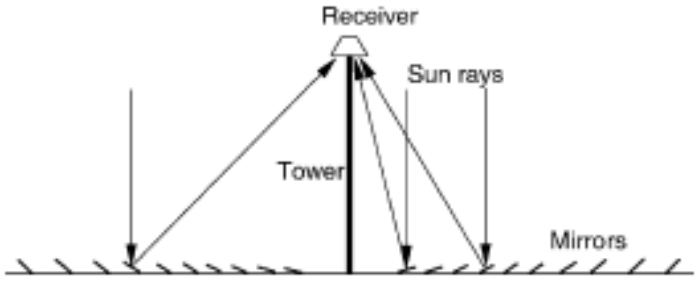

Figure 2.10: Schematic of LFR design [9]

Main drawback of the LFR technology is the blocking of sunlight by the adjacent reflectors. This needs to increase the spacing between the mirrors thus increasing the land usage. As a solution to this problem the compact linear Fresnel reflector (CLFR) technology has been introduced [7]. The two adjacent mirrors in the CLFR design are oriented towards two receivers in opposite direction with compact reflector field. Reflectors near the base of the receiver are oriented towards the same receiver [7]. So that the mirrors can be placed closer without blocking them by each other. Figure 2.11 is an illustration of the technology. LFR is the most efficient technology in land usage which is around 4 – 6 m^2/MWh/year. However it requires a ground with level with slope tolerance less than 1 degree [7].

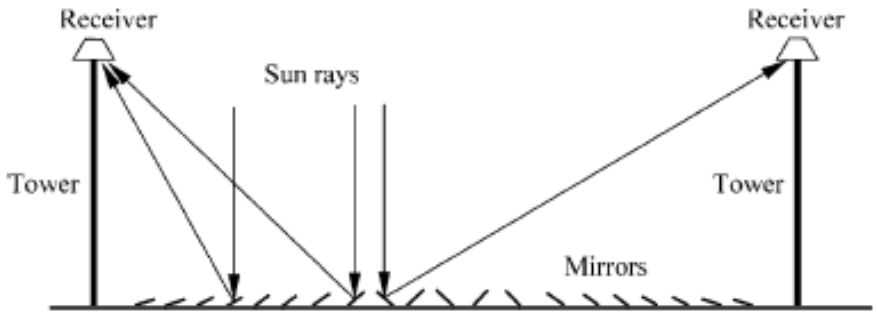

Figure 2.11: The design of CLFR system [9]

High number if flat mirror segments require complex control system with individual drive units. This is one reason that the system is not popular in large scale. The capital cost for the LFR is about 5700 – 6400 $/kW [18]. The operation and maintenance cost is low compared to PTC plants.

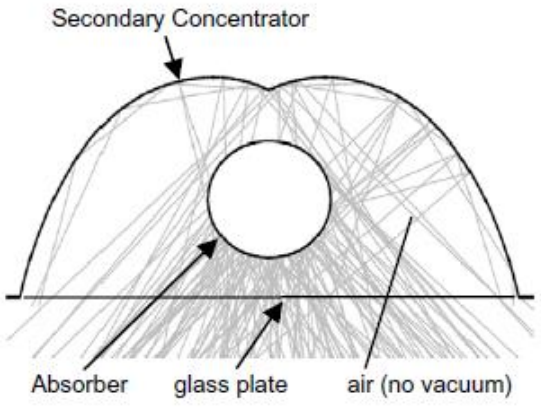

Figure 2.12: Secondary reflector of CLFR [12]

A secondary concentrator is fixed at the receiver to direct all the reflected radiant energy in to the absorber tube which are directed towards the receiver by the mirrors. Figure 2.12 shows the arrangement of absorber inside the secondary concentrator of CLFR technology.

2.2.4 Parabolic dish collector

Parabolic dish collectors concentrate solar rays to the focal point of the paraboloid where the receiver is located. In some concentrators the paraboloid shape of the

reflector is made with multiple spherically shaped mirrors supported on the structure. Figure 2.13 shows the parabolic reflector and the receiver for this technology.

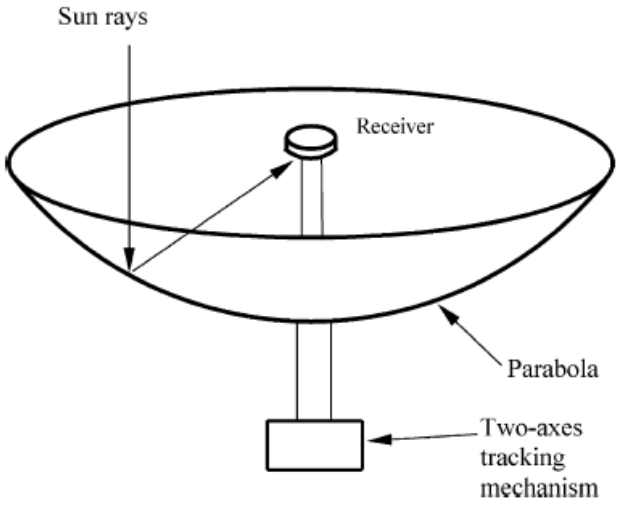

Figure 2.13: Schematic of parabolic dish collector [9]

At the receiver a Stirling engine is most commonly used to convert the heat energy in to mechanical energy which is fed in to an electric generator. Working fluid which is hydrogen or helium in most of the units is heated and pressurized in the solar receiver to power the engine [6]. This technology is equipped with two axes tracking mechanism for the parabolic reflector.

The receiver of this unit is a semi-circular shaped air cavity with absorber tubes laid on inner surface. This unit is encased with insulating material and the Figure 2.14 illustrates the cavity receiver fixed at the focal point of the dish.

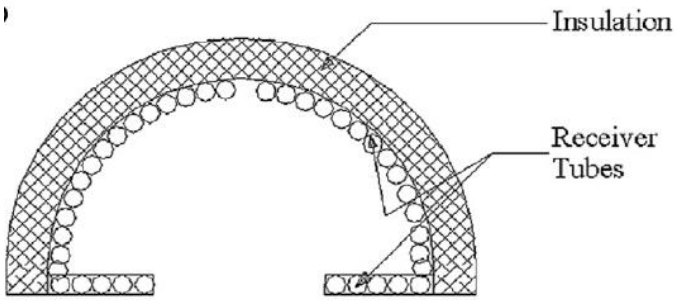

Figure 2.14: The cavity receiver of PDC plant [7]

Capacities of the PDC plants are in the range of 0.01 to 0.4 MWe [8]. With the capacities of this level these units seems to be suited for stand-alone power plants. Concentration ratio of PDC units are in the range of 1000 - 3000 suns [8]. Since the dish reflector is always pointed towards the sun system can achieve highest optical efficiency among the CSP technologies which is 94% [10]. Also the solar to electricity conversion efficiency is in the range of 25 to 30% [8]. The operating temperatures are over 1000 ^{o}C and the pressure range is between 40 bar and 200 bar.

The capital cost of the prototype PDC plants are higher compared the other technologies it is recorded as 12578 $/kW [8]. With the recent designs the capital cost is expected to drop to a level around 9000 $/kW [10]. The cost is approximately distributed as 40% for the concentrator mirrors and their controls, 33% for the energy conversion unit and 27% for the balance of plant and installation [9]. Mirrors are the major contributor to the high cost and it is around 80 to 150 $/m^2 [10]. A new low cost introduction for the mirrors in the pilot projects is to use stretched aluminium silvered polymer at a rate of 40 to 80 $/m^2 [10].

This technology does not require level ground as in the other technologies such as PTC and LFR. The land usage for the PDC is recorded as 8 – 12 m^2/MWh/year [8]. Another key benefit of this technology is that it does not use water for the operation.

2.2.5 Solar chimney plant

In this technology a tall vertical tower is located at the middle of large collector roof open at the periphery. The roof of collector is made out of glass or plastic and supported on a frame which is about 2 m in height above the ground level. Ground and air under the collector roof is heated by the solar radiation which passes through the transparent or translucent roof. Due to the natural and forced convection, heated air under the roof flows at high velocity towards the tower and then moves up through chimney. The velocity of the updraft air is approximately proportional to the temperature rise and the tower height [13]. The height of the glass roof increases near the tower, so air can divert to its vertical movement with low friction. As the air flows in to the chimney the wind turbine located at the centre of the chimney rotates and

thus the coupled generator produces electricity. Figure 2.15 illustrates the working of solar chimney plant.

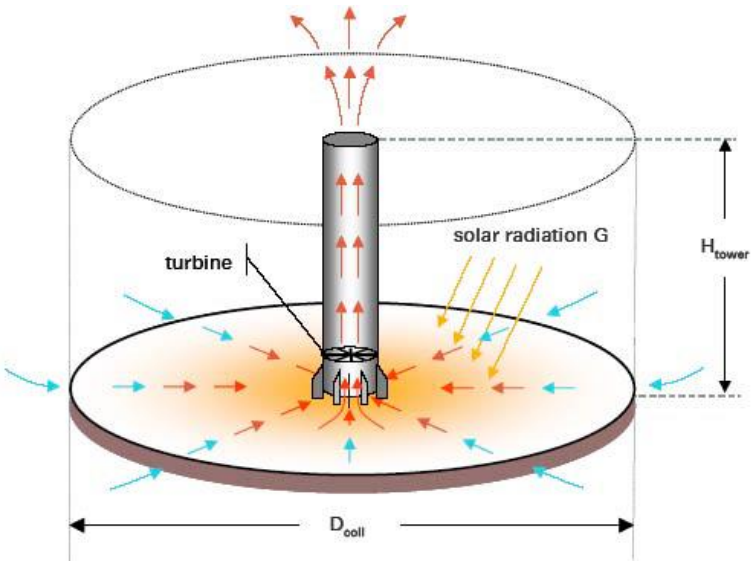

Figure 2.15: Solar chimney principle [6]

The power output from the turbine is proportional to the volume flow rate of air and the pressure drop across the turbine. Turbine blade pitch is adjusted during operation to regulate power output due to varying air speed and flowrate. Solar to electricity conversion efficiency of this technology is less than 2%. Therefore this technology is more suitable for the areas where the land is very cheap or free. So it is more suitable for desert areas. However the outer area under the collector roof can be used as green house for agricultural purposes in other regions.

A 200 m high prototype plant of this type was constructed in Manzanaraes, Spain. The radius of the collector roof is 122 m and it produces 50 kWe power output at peak [13]. Plant should be built in several megawatt range for the operations to be economical.

2.3 Comparison of CSP technologies

Concentrating solar power plants uses different technologies for collecting solar thermal energy to generate electricity. Variety of technologies and their fast

development makes it difficult to select which technology is best suited for a given condition. The selection become further complicated since there are several factors to be considered under technical, financial and environmental aspects. When comparing the different technologies, each has their own advantages and disadvantages.

PTC is the most widely adopted CSP technology, so it is well commercially proven for grid connected electricity generation. Also the performance data are widely available for this technology. But for the other technologies some data has been taken from the prototypes and theoretical predictions for the comparison. The variability of the plant performance depending on the solar radiation of the site is also an issue when summarizing the data. So that most of the data available as a range of values.

Table 2.1: Technical performance data of CSP technologies

Technology	**Capacity (MWe)**	**Solar – Electric conversion Efficiency (%)**	**Collector Efficiency (%)**	**Concentration Ratio**
Parabolic Trough	10 – 200 [8]	10 – 15 [8]	63 [10]	70 – 80 [8]
Heliostat field	10 – 200 [8]	20 – 35 [8]	72 [10]	300 – 1500 [7]
Linear Fresnel	10- 200 [8]	8 – 10 [8]	36 [10]	25 – 100 [8]
Parabolic Dish	0.01 – 0.04 [8]	25 – 30 [8]	66 [10]	1000 – 3000 [8]

Technical performance of the CSP technologies are summarized in Table 2.1 based on plant capacity, Solar – electricity conversion efficiency, collector efficiency and concentration ratio. PTC, HFC and LFR plants can be built in the capacity range of 10 to 200 MWe, while the PDC plant output is in kilo Watt range that is 10 to 400 kWe. Highest single unit capacities of PTC and HFC plants up to date are 80 MWe and 10 MWe respectively, and that is only 10 kWe for PDC plant. They can be combined in several units to achieve larger capacities. Since the unit capacity of PDC plants are low, they are much suitable for stand-alone, small off grid power systems

while the others can be connected to the grid. Conversion efficiency of solar energy to electrical energy is high in PDC plants compared to the other technologies even though their capacity is low.

Also it is noted that the concentration ratio of PDC and HFC technologies rather high compared to the others by heating heat transfer fluids to higher temperatures. Since HFC can operate at high temperatures, they are more suitable to work with Brayton cycle and combined cycle for power generation. Concentration ratios of LFR and CLFR are low while the latter shows little higher value than the first. Since this technology can produce steam around 300 ^{o}C, Rankine cycle with saturated steam is suitable for them. Rankine cycle with superheated steam can be used to get higher thermal efficiency compared to the previous in PTC plants since they can produce steam at 400 ^{o}C. A comparison of operating and stagnation temperatures as well as the operating cycles for the CSP plants are compared in Table 2.2.

Table 2.2: Operating conditions of CSP technologies

Technology	**Operating Temperature (^{o}C)**	**Stagnation Temperature (^{o}C)**	**Thermodynamic cycle**
Parabolic trough	20 – 400 [5]	600 [10]	Superheated steam – Rankine [4]
Heliostat field	300 – 565 [5]	1750 [10]	Superheated steam – Rankine [4]
Linear Fresnel	50 – 300 [5]	300+ [10]	Saturated steam - Rankine [4]
Parabolic Dish	120 – 1500 [5]	1200+ [10]	Stirling [4]

Capital cost, operation and maintenance cost and unit cost of electricity are considered for comparison as financial performance parameters. The information found from literature are summarised in Table 2.3. Among the CSP technologies PDC shows the highest capital cost since the cost of parabolic mirror dish and Stirling engine is high. Capital cost and operation and maintenance cost of PTC plants with direct steam generation is less compared to the PTC which uses synthetic oil as heat transfer

medium. Both capital cost and operation and maintenance cost is high in HFC plants compared to the PTC plants.

Table 2.3: Financial performance of CSP technologies

Technology	**Capital Cost ($/kW)**	**Capital Cost ($/m^2)**	**O & M cost ($/kWh)**	**Unit Cost ($/kWh)**
Parabolic trough	3900 – 8300 [18]	424 [8]	0.012 - 0.02 [8]	0.14 - 0.36 [19]
Heliostat field	5700 – 9000 [18]	476 [8]	0.034 [8]	0.17 – 0.29 [19]
Linear Fresnel	5700 – 6400 [18]	234 [8]	Low	-
Parabolic Dish	12578 [8]	-	0.21 [8]	0.16 – 0.22 [19]

Table 2.4: Environmental aspects and technology maturity

Technology	**Cooling water usage (m^3/MWh)**	**Land usage (m^2/MWh/year)**	**Technology maturity**
Parabolic trough	3 [4]	6 – 8 [8]	Very mature [7]
Heliostat field	2 – 3 [4]	8 – 12 [8]	Most recent [7]
Linear Fresnel	3 [4]	4 – 6 [8]	Mature [7]
Parabolic Dish	-	8 – 12 [8]	Recent [7]

When considering the environmental factors the CLFR technology has the lowest land requirement. HFC and PDC plants require comparatively larger land area even though they are flexible to build in areas which are not levelled. The cooling water requirement for PTC and LFR plants are relatively high when using wet cooling. Therefore such plants with wet cooling may not be suitable for the areas where the water availability is a problem. There is no cooling water requirement for PDC technology. Data related to land usage and cooling water usage are given in Table 2.4.

Also the level of maturity of different CSP technologies are shown in Table 2.4. According to the literature, PTC technology is the most matured CSP technology while HFC is the most recent.

2.4 Thermal Energy storage

One of the major problems with solar radiation as an energy source is its varying nature during the day and during the year. Seasonal weather changes also effected to the amount of solar energy that can be collected by the concentrators. This influences the plant efficiency, electricity generation cost and specific output. Solar radiation peaks at afternoon, but the electricity consumption peaks at evening. Therefore a reliable energy storage has to be employed with the CSP plant to have successful operation. In CSP plants Thermal Energy Storage (TES) serve multiple purposes. TES helps to balance the plant in transient periods. During overcast it enables the stable turbine conditions by supplying stored energy to the power block, hence the number of full load hours would be more. Energy stored in a thermal energy storage media during solar peak hours can be used at night time to run the turbine. The most important reason for implementation of large capacity TES is for the plant to be able to supply dispatchable or base load power to the grid and even stabilize the demand [15]. TES would increase the plant capital cost but when compared with the mechanical or chemical storage the cost is comparatively less. Also operating efficiencies of thermal storages are high compared to the other storage technologies. One of the main advantages of CSP is that it can be equipped with low cost thermal energy storage compared to solar photovoltaics.

The cyclic nature of solar energy suggests two types of energy storages, as short term energy storage and long term energy storage to have continuous operation of the plant throughout the year [7]. Short term TES is occupied to store the excess energy harvested during the day and use it in the night time. Long term TES is essential to store excess energy during summer and use it during winter season. The TES consists of a heat exchanger, cold tank, hot tank and control valves as shown in Figure 2.16. When excess heat is collected at the solar field, heat is transferred to the heat

exchanger. Then the HTF moving from cold tank to hot tank is heated there. Heat can be transferred back to heat transfer fluid from hot tank when needed.

There are two ways of achieving TES as direct method and indirect method. Direct method heat up liquid medium such as synthetic oil, mineral oil, silicone oil or molten salts directly to store energy as sensible heat. High density, low vapour pressure, moderate specific heat, low chemical reactivity and low cost are the desired characteristics for direct energy storage mediums [5]. In the indirect method, the storage material is a solid medium which is heated by the absorbed heat of HTF. Reinforced concrete, cast iron, cast steel, NaCl crystals and silica fire brick are suitable solid mediums for TES [4].

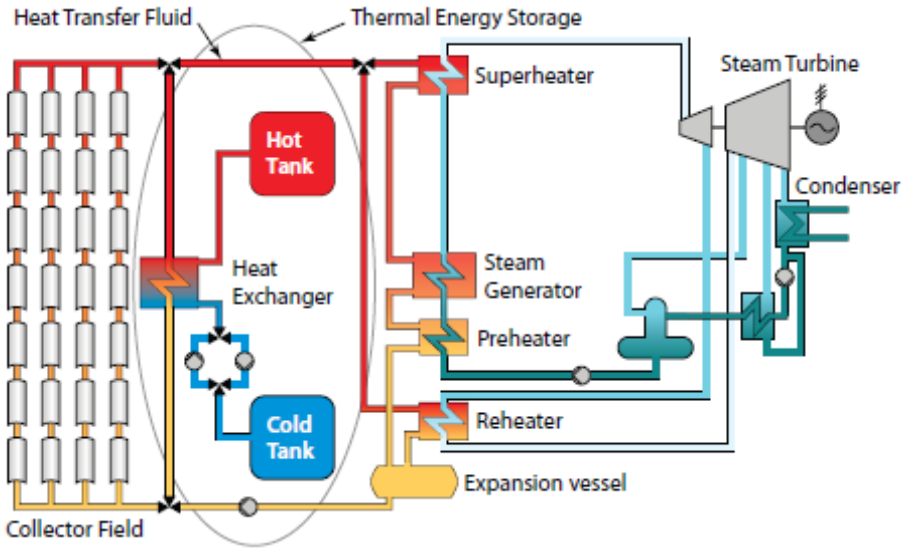

Figure 2.16: CSP plant with thermal energy storage [4]

Energy can be stored in storage medium in two ways as sensible and latent energy. Sensible heat storage is heating of solid or liquid and insulating it from the environment until use. Phase change from solid to liquid or solid to vapour of storage material is considered as latent heat storage. The reason to prefer solid to vapour phase change over liquid to vapour phase change is its low volumetric expansion. The latent heat storages can store significantly higher amount of heat at constant temperature compared to sensible heat storage. The storage capacity of latent heat storage is governed not only by the specific heat capacity but also by the latent heat of phase

change of the material. This leads to a smaller, low cost and efficient storage compared to sensible storage [4]. Sodium nitrate, sodium nitrate/potassium nitrate mixture, lithium carbonate and sodium carbonate mixture are some of the tested materials for latent energy storage [4].

2.5 Backup systems

CSP plants with or without energy storage commonly equipped with backup systems. Usually backup unit is a fossil fuel fired burners. This helps to regulate the power output form the plant nearly at a constant value. Fuel burners provide energy to the heat transfer fluid or to the storage medium. In some arrangements backup burners supply energy directly to the power block by producing steam at a backup boiler. The CSP plants with a backup system usually called as hybrid plants since they use solar thermal and fuel to produce power. A small solar field can be added to a fossil fuel fired power plant also. This has been done only to limit the fossil fuel usage.

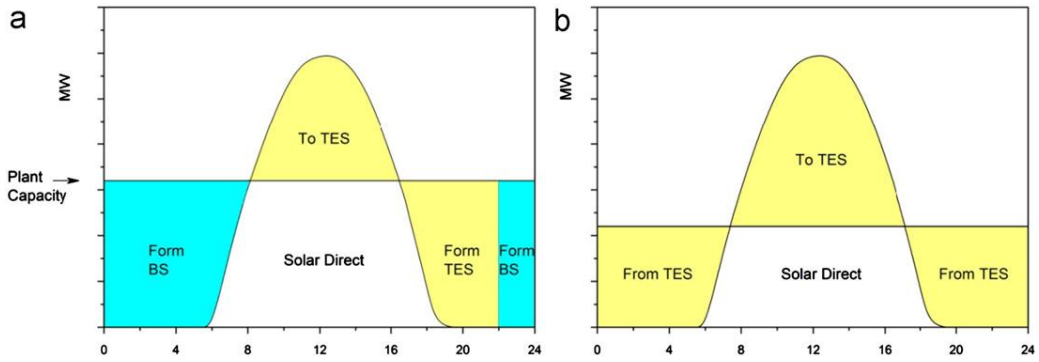

Figure 2.17: CSP plant performance with TES and backup (a) and sole TES (b) [5]

A CSP plant with Backup system and TES can operate at higher capacity throughout the day than a plant only with storage. The plant operate at its full capacity during the daytime while storing the excess energy in TES. The storage supplies energy to power up the plant during early night and then the backup system start to operate at late night to maintain constant power output throughout the day. Figure 2.17 illustrates how the plant capacity has been increased with the introduction of backup system with a TES to a CSP plant.

2.6 Heat Transfer Fluids

Heat transfer fluids are used to absorb the concentrated solar energy at the receiver and then transport it to the power block and thermal energy storage. Other than the CSP plants which uses direct steam generation, all the plants are equipped with heat exchanges of suitable capacity to exchange heat with the working fluid (water or air) of the power cycle. Suitable HTFs for the application should be thermally stable at high temperatures and should have high thermal capacity, low vapour pressure, low freeze point, low toxicity, low explosivity and low environmental hazard properties. The fluids must be easily available at low cost. Suitable fluids must be chemically compatible with contact material in order to prevent the effects of corrosion of contact surfaces [6] [15].

Table 2.5: Properties of commonly used HTFs

HTF	Type	Minimum operating temp.(ºC)	Maximum operating temp. (ºC)	Freezing Point (ºC)
Hitec solar salt	Nitrate salt	238	593	238
Hitec	Nitrate salt	142	538	142
Hitec XL	Nitrate salt	120	500	120
Therminol VP-1	Mixture of Biphenyl and Diphenyl Oxide	12	400	12 (crystallization point)
Therminol 59	Synthetic oil	-45	315	-68 (pour point)
Therminol 66	Synthetic oil	0	345	-25 (pour point)
Caloira HT 43	Mineral Hydrocarbon	-12	315	-12 (pour point)
Downtherm Q	Synthetic oil	-35	330	n/a

Source: SAM library

HTFs with high density and high heat capacity can be used as storage mediums as well. If the thermal conductivity of the fluid is high, its temperature become closer to receiver temperature. Fluids which has low viscosity requires low pumping power [15]. Synthetic oil and nitrate salts are the most commonly used substances as HTFs in CSP plants and some of their properties are displayed in Table 2.5. With the use of

HTF the system can operate at high temperatures, which is above 500 ^{o}C. Due to that the Rankine steam cycle operates at high temperature leading to high thermal efficiency.

2.7 Future cost of CSP plants

Total installed cost of CSP plants with storage is higher than the plants without storage. But thermal energy storages allow the plants to increase their capacity factors by producing energy using the stored energy during the period where there is no sunshine. Total installed plant cost for parabolic trough systems without storage range between USD 3900/kW and USD 8300/kW [18]. Adding 4 to 8 hours of storage will increase the installed cost in the range between USD 6050/kW and USD 13150/kW [17].

It is estimated that the learning rate, that is the reduction in cost for every doubling of cumulative capacity for the period 2010 to 2022 could reach 30% [17]. It is expected that the capital cost of CSP will decline by around 30% to 50% in 2020 [18]. Improvements in CSP technology is the key factor for cost reduction. The continuous technological innovation has reduce the cost of equipment such as collectors and mirrors and improve their performance. These improved performance also leads to a reduction in maintenance costs. Technological improvements has reduced costs in installation and engineering. Competitiveness among the large number of experienced project developers is also would lead to the reduction in cost. The CSP technology is also expected to experience a decline in its indirect costs and the owner's cost elements as well.

The operation and maintenance costs are also a significant component of the overall Levelized Cost of Energy (LCOE) of CSP projects. These costs mainly include the cost for replacement of mirrors and receivers, and cost of mirror washing. The Solar Energy Generating System plants that were built between 1982 and 1990 were estimated to have operation and maintenance costs around USD 0.04/kWh [17]. Advances in materials and new designs with the technology development has reduced the mirror and receiver breakages leading to a significant reduction in operation and maintenance costs. It is estimated that these costs to be in the range of USD 0.02/kWh

to USD 0.04/kWh for the proposed projects including insurance [17]. The overall cost reduction potentials for operation and maintenance costs could be in the range of 35% for parabolic trough plant and 23% for heliostat solar power tower plants by 2020 [19].

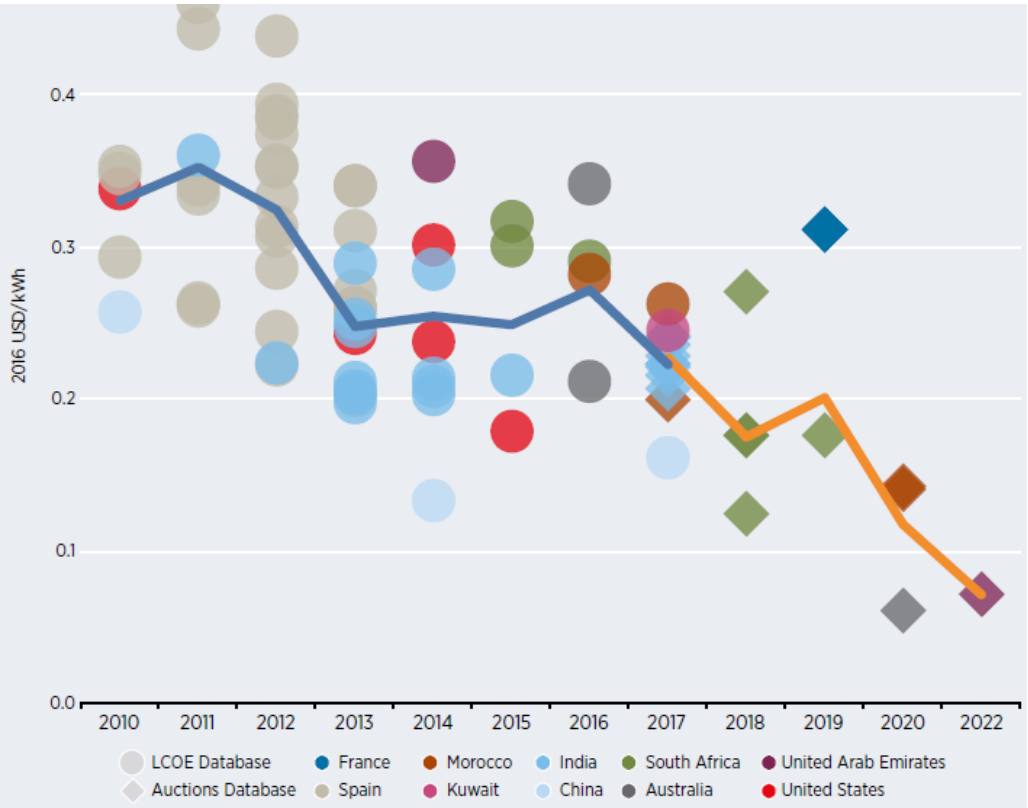

Figure 2.18: LCOE and auction price trend for CSP, 2010 – 2022 [17]

Level of DNI and the plant cost are the main components that decides the value of LCOE. High level of DNI is likely to the main driving factor of lower LCOE during the period 2009 to 2012 [17]. The reduction in installed cost and operation and maintenance cost is also lowered LCOE in CSP generated electricity in recent past. With the introduction of thermal storage, the plant capacity factors were increased while reducing cost of energy. The LCOE of most projects in the period 2014 to 2016 is below USD 0.30/kWh [17]. During 2016 the capacity weighted average LCOE of CSP plants was estimated to be USD 0.27/kWh. The International Renewable Energy Agency (IRENA) data suggests that the LCOE of CSP generated electricity during 2017 is USD 0.22/kWh [17]. Recent announcement and analysis of planned projects

seems to predict a clear downward trend in cost of energy. Some examples are USD 0.073/kWh bid announced by Dubai Electricity and Water Authority and USD 0.06/kWh bid for Port Augusta CSP project in Australia [17]. For CSP, year 2016 and 2017 have been breakthrough years, as auction results around the world have confirmed that a step change in costs has been achieved and will be delivered in projects commissioned from 2020 onwards could fall in the range USD 0.06/kWh and USD 0.10/kWh [17]. Figure 2.18 shows the trend of LCOE over the years.

It is noticed that the increased competitiveness of renewable energy projects compared to fossil fuel alternatives and that by 2020 commissioned CSP plants will increasingly be delivering electricity at a cost that is within the lower end of the fossil fuel fired cost range.

2.8 Simulation software tools for CSP plants

A software tool has to be used to simulate the technical and financial performance of the CSP plant at the selected location. System Advisor Model (SAM) and TRNSYS are most commonly used software tools for the simulation of CSP performance. Both the softwares can be used as modelling tools for renewable energy projects. SAM is a freely available software which was developed by National Renewable Energy Laboratory (NREL). TRNSYS is commercially available software which was developed at the University of Wisconsin, Madison, and is maintained by several distributors, including researchers at the University of Wisconsin [20]. TRNSYS is capable of constructing complete models of power systems. User defined modular components can be connected together to model a total system. The components consists of solar thermal collectors, heat exchangers, thermal storage tanks, hydraulics, power cycles and controllers [20].

Compared to TRNSYS, a high performance transient time series solver frame work has been implemented in the current simulation engine for CSP models in SAM [21]. When modelling the CSP systems, a very low root mean square deviation is shown by the two softwares, SAM and TRNSYS. SAM provides a significant reduction in computation time relative to TRNSYS [21].

SAM software can be used to predict the technical and financial performance of grid connected electricity generation projects. These projects can be either on the customer side of the utility meter or on the utility side of the meter [22]. For the first type they buy and sell electricity at retail rates and for the second type they sell electricity at a negotiated price through a power purchase agreement [22].

SAM software can be used mainly to estimate energy output and cost predictions of a power generation project. The software can be used as a simulation tool for solar thermal, solar photovoltaics, wind, geothermal and bio mass power projects as well. And also SAM can be used to model solar water heating projects.

2.9 Solar Irradiation of Sri Lanka

Sri Lanka has already introduced solar PV technologies for electricity generation to cater its increasing energy demand. If the country can adopt CSP technologies in future it will also helpful to achieve the future targets that they are planning to achieve in renewable energy sector. A good quantitative knowledge of the distribution and extent of solar resources in Sri Lanka is essential in order to make appropriate decisions on the applications of solar technologies [23]. Hence the designers will be able to properly size the systems being designed in order to meet loads and to attract further investments in these technologies.

Since CSP plants can be operated with the direct solar radiation it is necessary to identify the areas which has high direct radiation in the country. According to the DNI map of Sri Lanka presented in Figure 2.19, areas such as Kilinochchi, Hambanthota, Mannar and Eastern coastal regions have high level of direct radiation. Most of the areas of the country has annual DNI level of less than 1450 kWh/m^2.

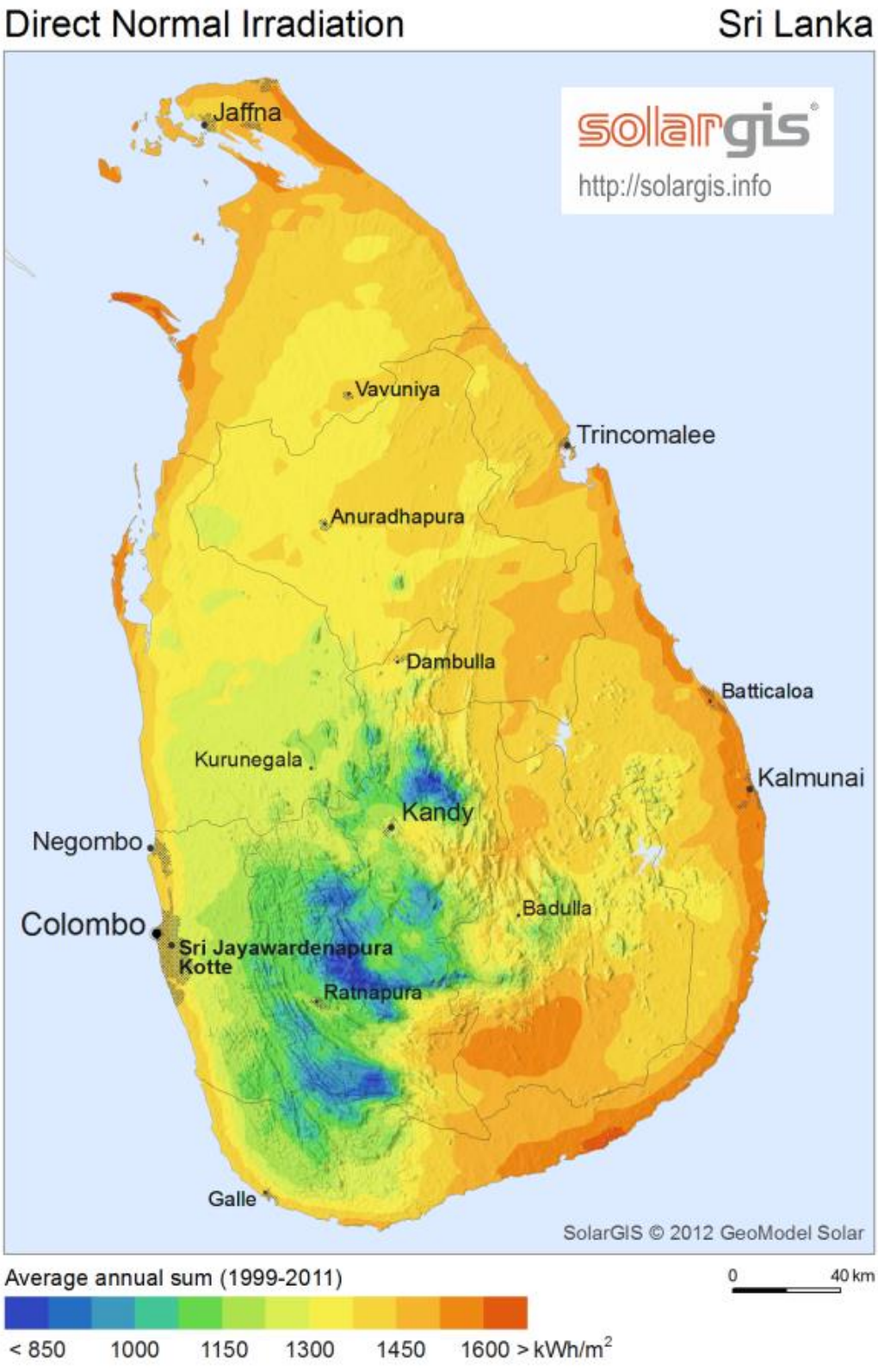

Figure 2.19: DNI map of Sri Lanka [25]

DNI data from Solar and Wind Resource Assessment Programme (SWERA) for different locations in Sri Lanka are provided in Table 2.6. These high resolution solar radiation assessment is based on data of geostationary satellite Meteosat [24]. Hambanthota and Batticaloa are having annual DNI levels over 1600 kWh/m^2.

Table 2.6: DNI data of Sri Lanka

Location	**DNI (kWh/m^2/day)**	**DNI (kWh/m^2/year)**
Hambanthota	4.51	1646
Batticaloa	4.39	1602
Trincomalee	4.21	1537
Kankesanthurai	3.99	1456
Puttlam	3.86	1409
Anuradhapura	3.86	1409
Katunayake	3.68	1343
Rathmalana	3.58	1307

Source: SWERA

3 THEORY

3.1 Concentration Ratio

Concentration ratio is the parameter that describes the amount of solar energy concentration achieved by the particular type of collector. The most commonly used definition of the concentration ratio, is an area concentration ratio. It is defined as the ratio of the area of the aperture to the area of the receiver [26].

The area concentration ratio, C

$$C = \frac{A_a}{A_r}$$

Where A_a is the aperture area and A_r is the receiver area.

This area concentration ratio can be related with the heat losses in the concentrator since it refers to receiver area. Heat losses at the receiver is high since its temperature is high. A common way of reducing the heat losses at the receiver is to reduce its area. By reflecting or refracting the radiation incident on a large collector aperture area on to an absorber of smaller area, concentrating collectors reduce the area of the receiver. With the reduced heat loss, these collectors are able to operate at high temperatures and provide greater amount of useful thermal energy. Heat losses from the collector are almost proportional to the absorber area. Hence it is inversely proportional to the area concentration ratio [27].

The optical or flux concentration ratio is defined as the ratio of the average energy flux on the receiver to that on the aperture [26]. This directly relates to the reflector quality. Optical and geometric concentration ratios are equal when receiver irradiance and aperture insolation are uniform over the entire area.

To deliver energy at higher temperatures, the concentration ratios should be high for the collectors as shown in figure 3.1. The concentration ratios when energy absorbed is equal to the thermal losses are represented in the lower limit curve. Higher concentration ratios then result useful energy gain. Collector efficiencies of 40% to 60% are represented in the shaded region which is the range of operation in practice [26].

A parabolic trough collector captures solar radiation over a large aperture area. It concentrates this energy on to the absorber which has much smaller area. Concentration ratio for parabolic trough systems in the range of 10 to 80 [26]. The collectors need to track sun throughout the day time to achieve efficient energy collection.

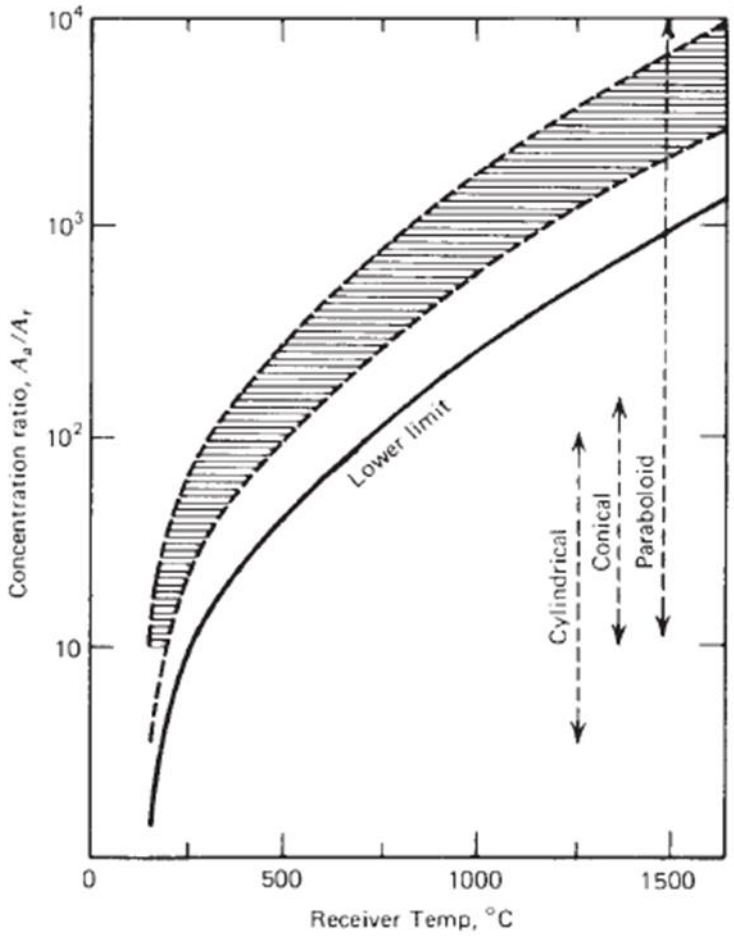

Figure 3.1: Relation between receiver temperature and concentration ratio [26]

3.2 Useful Energy Collected

The useful energy collected by concentrating collectors can be obtained by considering the energy balance of the system. The thermal energy analysis of a flat plate solar collector and a concentrating collector are similar [26]. From the

generalized thermal energy analysis, the useful energy collected by the concentrating collector (Qu) is given by,

$$Q_u = F_R - A_a[S - \frac{A_r}{A_a} U_L(T_i - T_a)]$$

Where,

F_R is the collector heat removal factor

U_L is the heat loss coefficient

S is the solar radiation absorbed

A_a is the aperture area

A_r is the receiver area

T_i is the fluid inlet temperature

T_a is the atmospheric temperature.

With the known values of F_R and U_L the collector useful gain can be calculated.

3.3 Levelized Cost of Energy

The levelized cost of energy captures the tradeoff between the benefit of higher annual electricity output and the cost of increased capital expenditures associated with the plant. Some factors that governs the value of LCOE are the type of technology, capital cost, operating cost and the renewable energy resource [19]. Different technologies of energy production in different scales of operation, different investment and operating time periods can be compared using LCOE [28].

By definition, the projects annual cost is the product of LCOE and electricity generated in that year.

$$C_n = LCOE \times Q_n$$

The formula for calculating LCOE is,

$$\text{LCOE} = \frac{\sum_{n=0}^{N} \frac{C_n}{(1+d)^n}}{\sum_{n=1}^{N} \frac{Q_n}{(1+d)^n}}$$

Where,

Q_n = Electricity generated by the system in year n

N = Analysis period in years

C_0 = Projects equity investment amount

C_n = Annual project costs in year n

d = Discount rate

4 METHODOLOGY

A literature survey was done in order to study and compare the different technologies available to capture the solar thermal energy. In addition the solar irradiation data in different locations of Sri Lanka was compared with minimum DNI levels required for effective operation of a CSP plant. Further the study was extended to find out a suitable software for simulating a model of a CSP plant.

With the findings of the literature review it was decided to select Parabolic Trough technology as the most suitable technology for the country. Followings were the reasons for taking the decision.

- Most matured among the CSP technologies
- Commercially well proven technology
- Suitable for grid connected systems
- Capital cost is comparatively low

It was decided to select Hambanthota as the location for the plant since it has the highest annual DNI level. A software simulation was performed for a parabolic trough CSP plant of capacity 10 MWe. SAM version 2017.9.5 was used as the simulation tool. Two models as physical trough and empherical trough model are available in the software. In the physical trough model many of the plant components has to be designed using the first principles of thermodynamics and heat transfer [29]. The empherical model is based on empherical measurements taken from the existing plants [29]. Empherical trough model was used as the performance model in this study. Single owner utility model with a power purchase agreement (PPA) was selected as the financial model. Number of inputs were fed in to the input pages of the selected model including weather data of the location, solar field data, power block details, thermal storage characteristics, cost values and financial parameters.

4.1 Location and Resource

Location and resource page of SAM provides the opportunity to the user to select location of the plant need to be studied and its weather data from a suitable source. There are three options available in the software to get solar and weather data of the

location. Weather files can be downloaded from NREL's National solar radiation database. The other option is that to use solar resource library of the SAM software and select data file for the selected location. A specific weather file saved in the disk also can be used for the simulation. Weather files from different sources are available for different locations of the world. National Solar Resource Data Base (NSRDB), Solar and Wind Energy Resource Assessment Programme (SWERA), The ASHRAE International Weather for Energy Calculation version 1.1 (IWEC) and Canadian Weather for Energy Calculations (CWEC) are the sources of weather files available in the software library. For SAM library the SWERA programme provides the weather data for different locations in Sri Lanka.

Required weather data for Hambanthota including hourly values of DNI, wind speed and dry bulb temperature are available in the SAM library. Those values from the weather files of SAM library were used for this simulation. Figure 4.1 shows the hourly variation of DNI and temperature at Hambanthota. Details of the selected location and a summary of weather data are displayed in Table 4.1.

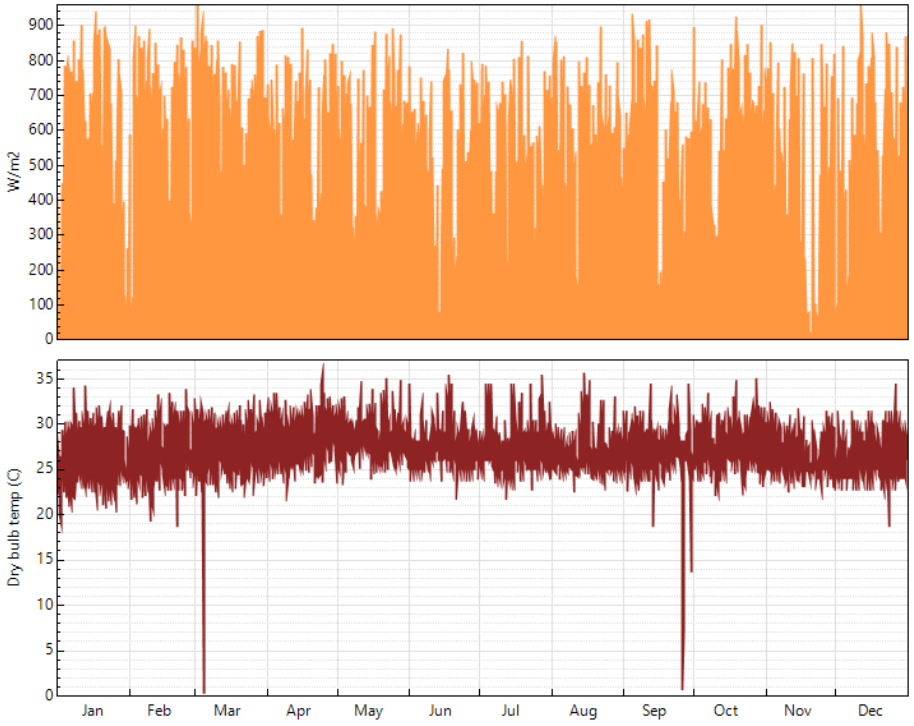

Figure 4.1: Hourly variation of DNI and temperature at Hambanthota

Table 4.1: Location and annual weather data summary for Hambanthota

Parameter	Value
Latitude	6.12 ^{o}N
Longitude	81.13 ^{o}E
Direct Normal Irradiation (kWh/m^2/day)	4.51
Diffuse radiation (kWh/m^2/day)	2.40
Average temperature (^{o}C)	27
Average wind speed (m/s)	5.6
Elevation (m)	20

Source: SAM library

4.2 Solar Field

The solar field page of the software displays the variables and provides different options related to the solar field design. It also includes the types of heat transfer fluids, their properties, reference design specifications and collector orientations. There are two options available in SAM software as solar multiple (SM) mode and solar field area mode. A value for solar multiple has to be specified in solar multiple mode and the software automatically calculates the solar field area based on the fixed power block capacity. A value for solar field area has to be specified and software calculates the solar multiple in the other mode. In this option the power block capacity has to be adjusted manually to match the solar field output. Solar multiple mode was selected for this simulation since it is more convenient to assume a set of values for solar multiple and select the most suitable value with parametric simulation rather than assuming the solar field area for the fixed power block capacity of 10 MWe.

4.2.1 Solar Multiple

Solar Multiple 1 (SM = 1) is the solar field area required to deliver sufficient solar energy to drive the power block at the design turbine gross output level under reference weather conditions [16]. This has been calculated using the reference conditions of weather data the ambient temperature, wind velocity and DNI. As the reference conditions DNI was taken as 940 W/m^2/day, which was the maximum in the site. The annual average values were taken as the reference values for ambient

temperature and wind velocity. The reference ambient temperature was 27 ^{o}C and the reference wind velocity was 5.6 m/s for Hambanthota. Solar multiple is used to calculate the exact aperture reflective area of the solar field required as shown in below equation [16].

Aperture Reflective Area = Solar Multiple × Exact Aperture Reflective Area at SM=1

With a higher value of solar multiple higher annual energy output can be obtained since the solar field area increases with SM. The plant capital cost increases with the solar field area. Therefore the financial performance parameters were compared at different solar multiple values in order to find out an optimum value for the solar multiple. Optimum solar field area for the location which minimizes the LCOE was found by varying the solar multiple. For a range of solar multiple values from 1 to 5 with the intervals of 0.5, the annual energy generation of the plant, LCOE and Internal Rate of Return (IRR) were obtained.

4.2.2 Heat Transfer Fluid

Heat transfer fluid absorbs heat at the heat collector elements and transport energy to power block or to thermal storage. The software includes several heat transfer fluids in its library. Using these available heat transfer fluids, a parametric simulation was performed in order to find out most economical type of HTF. Annual energy generation, LCOE and IRR has been used as performance parameters against the different types of HTFs in the simulation.

Solar field inlet and outlet temperature values were taken as 220 ^{o}C and 320 ^{o}C respectively and were well within the operating temperature range of selected HTF. Solar field initial temperature was kept at 100 ^{o}C. Piping heat loss at design temperature was 10 W/m^2 which was the default value specified for the empherical model. Piping heat loss coefficients and capacity of HTF per area were also kept at the default values.

4.3 Solar Collector Assembly

Solar collector assembly is an individual solar energy tracking component which includes the mirrors, supporting structure and receivers. The solar field consists of

number of SCAs. In the empherical model of the parabolic trough plant, a pre designed SCA can be selected from the SAM library. The SCA input variables describe the geometric and optical parameters of the collectors. Length, width, reflective area, focal length and incident angle modifier factors are the available geometric parameters. Mirror reflectance and mirror cleanliness are among the important optical parameters. Some of the major properties of different SCA types available in the SAM library are listed in Table 4.2. All the parameters were defined for each type of SCA and the user does not need to specify any of them.

Table 4.2: Major properties of available SCA types

Type	**Length (m)**	**Width (m)**	**Area (m^2)**	**Focal length (m)**	**Mirror reflectance**
Euro Trough ET 150	150	5.75	817.5	2.1	0.935
Luz LS-2	50	5	235	1.8	0.935
Luz LS-3	100	5.75	545	2.1	0.935
Solargenix SGX-1	100	5	470.3	1.8	0.935
Albiasa Trough AT150	150	5.77	817.5	1.71	0.935
Siemens SunField 6	95.2	5.78	545	2.17	0.925
SkyFuel SkyTrough	115	6	656	2.15	0.930
FLABEG Ultimate	247	7.53	1720	2.38	0.940

Source: SAM library

The distance between solar collector assemblies (SCA) was kept at the default value of 1m. It is the end to end distance between SCAs in a single row while assuming that all of them were laid out uniformly in the solar field. The centerline to centerline distance between the rows of SCAs was 15m as set by the software default. Number of SCAs per row was taken as 4. Deploy angle and stow angle were kept at the default values of 10 degrees and 170 degrees respectively. The collector angle from horizontal was zero degrees. Collectors were assumed to be fixed along North - South axis with zero degrees azimuth. The values of the above angles were used to calculate the incidence angle and the tracking angle in the simulation process by SAM. The non-solar field land area multiplier was kept at 1.4 as given in the software default values.

A series of simulations with different available SCAs were performed to select the best one for the application. Annual energy generation, LCOE and IRR were used to select most suitable type of SCA for the plant under the study.

4.4 Heat Collection Element

Heat energy receivers can be modeled under different conditions by varying the receiver variables that describe their properties. There are four different states of HCEs available in the empherical model of SAM software that specifies the different conditions of them. Vacuum, lost vacuum, broken glass and hydrogen are the four different states of available HCEs. Vacuum refers to the HCEs in good condition which is the major proportion. Others are lost vacuum, broken glass and hydrogen refer to different problem conditions in minor proportion. For this simulation 99.5% of HCEs in good condition and 0.5% of them in broken glass condition was assumed.

With the library values of optical parameters software calculates the optical efficiency of the receivers as in the following equation [16].

Optical Efficiency = SCA Field Error × Dust on Envelope × Bellows Shadowing × Envelope Transmissivity × Absorber Absorption × Unaccounted

There are four different types of HCEs available in the SAM library to select. The default 2008 Schott PTR70 Vacuum with transmissivity 0.963 and absorption 0.96 is used for the simulation. All the optical parameters and heat loss parameters were set at the default values.

4.5 Power Block

Parameters in the power block page describe the equipment used to convert thermal energy in to electrical energy. The power block operates on a steam turbine. The steam power plant runs on a Rankine power cycle. No fossil fuel back up is included for this plant.

This simulation was performed for a power plant of capacity 10 MWe. Therefore the design gross output was taken as 11 MWe and the gross to net conversion factor of 0.9 was assumed due to the parasitic losses. The value of design gross output value

was used to calculate the size of the solar field by software. The estimated gross to net conversion factor is the ratio between the electric power supplied to the grid and gross power output of the power block. A constant value of 4% is considered for availability and curtailment losses.

A suitable reference system turbine has to be selected form the power cycle library of the SAM software for the simulation. This includes five different types of conventional Rankine cycle steam turbines. Heat is transferred from HTF to water in a heat exchanger to generate steam that drives the turbine.

Table 4.3: Reference system turbine details

Reference System	**Power output at design (MWe)**	**Rated conversion efficiency (%)**	**Solar field size (m^2)**	**Operating temperature (^oC)**	**Suggested modelling application**
SEGS 30 MWe	30	37.49	180,000 – 230,000	300 - 400	Typical applications
SEGS 80 MWe	80	37.74	460,000 – 480,000	400	Typical applications
Nexant 450C HTF	100	39.57	-	450	High temperature HTF (molten salt)
Nexant 500C HTF	100	40.76	-	500	High temperature HTF (molten salt)
Siemens 400C HTF	50	37.36	-	400	High temperature HTF
APS Ormt 1MWe	1	20.71	10,000	300	Organic Rankine cycle power block

Source: SAM library

Capacity of the available turbines in the reference SAM library varies from 30 MWe to 100 MWe and their operating temperature range varies between 300 ^{o}C and 500 ^{o}C and their details are shown in Table 4.3. In addition to the data present in Table 4.3 the part load thermal to electric factors, factors of maximum turbine overdesign operation and factors of minimum turbine operation are available for each of the reference system in the library.

SEGS 30 MWe turbine was selected from the power cycle library as the reference system for this simulation since it is within the design capacity, selected temperature and the size of the solar field for 10 MWe plant. As per the library values the rated cycle conversion efficiency is 37.49% for the selected turbine. The fractions of the design point for the maximum turbine over design operation and minimum turbine operation are 1.15 and 0.25 respectively.

4.6 Thermal Storage

4.6.1 Thermal Energy Storage

The capacity of the thermal energy storage of a CSP plant is expressed in number of hours. The number of hours of storage times the power block design thermal input is the physical capacity of the TES. Higher storage capacities lead to higher annual energy generation and higher capacity factors. But on the other hand higher capacities of thermal energy storage lead to high capital costs. Therefore considering the financial performance parameters, an optimum value for thermal energy storage equivalent full load hours was obtained. Parametric simulation was performed in order to find out an optimum value for number of equivalent full load hours of TES.

The size of TES and solar multiple values are interrelated each other. When the size of solar field has increased it collects more energy, hence required more capacity at the storage to store energy. But on the other hand when the size of both TES and solar multiple has increased the capital cost will increase. Therefore an optimum combination of the above two parameters has to be decided. A parametric simulation was performed for this purpose by considering a set of solar multiple values in a range

of 1 to 5 at intervals of 0.5 and TES capacities from 0 to 10 hours at intervals of 1 hour.

The storage system consists of two tanks as cold storage tank and hot storage tank. It was decided to use same fluid as heat transfer fluid and thermal energy storage fluid. Since the same fluid was used, this system was a direct system without a heat exchanger between the thermal energy storage and thermal energy collection system.

4.6.2 TES dispatch control

The dispatch control system of TES determines the timing of energy releases from the storage. The software decides whether to operate the power block or not in each hour of simulation based on the dispatch control parameters set by the user. These parameters must be set based on how much energy is provided by solar field, how much energy is stored in the TES, and how much energy output is required. There are two targets for starting the power block in each period. One for periods of sunshine that is with solar (w/solar) and the other for periods of no sunshine that is without solar (w/o solar). Storage dispatch w/solar determines the minimum energy in storage at which the TES can deliver energy for daytime hours when the solar energy incident on the field is greater than zero. Storage dispatch w/o solar determines the minimum energy in storage at which TES can deliver energy for night hours when the solar energy incident on the field is zero. For each dispatch period, the turbine output fraction determines the load level of the power block in operation using the energy available in the storage. The load level mainly depends on the turbine output fraction and design turbine thermal input.

From mid night to early morning i.e. from 12.00 mid night to 6.00 am the storage dispatch factor was set to 1 and turbine output fraction was set to 0 since no power output was expected form the plant during that period. From 6.00 am to 6.00 pm the storage dispatch fraction was set to 0 so that the storage can dispatch maximum possible energy in to the power block when there are cloud transients. For this period the turbine output fraction was set to 1.15 which is the maximum and hence the plant can produce its maximum possible load. From 6.00 pm to 12.00 mid night the storage dispatch fraction was set to 0 and turbine output fraction was also set to 1, allowing

TES to dispatch maximum possible energy to the power block and the turbine to operate at its designed capacity.

4.7 Parasitic Energy

Parasitic electrical loads includes the energy consumption by drive motors, pump motors and electronic circuits. SAM software includes a set of default parasitic parameters for parabolic trough systems. The design point parasitic values are the maximum possible values for each loss category. Based on the design point, the hourly loss values were calculated by the software considering solar field thermal energy output and power block load in each hour. The default system SEGS VIII-Reference was used for the analysis. SAM library data of parasitic electric energy usage are shown in Table 4.4.

Table 4.4: Parasitic electric energy use

Parameter	Value
SCA drives and Electronics (MWe/m^2)	2.66e-007
Solar field HTF pumps (MWe/m^2)	1.052e-005
TES pumps (MWe/MWe)	0.02
Power block fixed	0.0055
Balance of plant (MWe/MWe)	0.02467
Heater and boiler (MWe/MWe)	0.02273
Cooling towers (MWe/MWe)	0.017045

Source: SAM library

4.8 System Costs

System costs page of the software includes the variables related to direct capital costs, indirect capital costs and operation and maintenance costs of the plant. Direct capital costs include the costs related to site improvements, solar field, HTF system, thermal energy storage, power plant and balance of plant. Default rates of the cost values were used for calculating the total direct cost for the plant and their values are shown in Table 4.5. A contingency allowance of 7% was imposed on above direct costs due to uncertainties in above cost estimates.

Table 4.5: Direct capital costs default values

Cost category	Value
Site Improvements ($/m^2)	26.00
Solar Field ($/m^2)	150.00
HTF system ($/m^2)	60.00
Storage ($/kWht)	65.00
Power Plant ($/kWe)	1150.00
Balance of Plant ($/kWe)	120.00

Source: SAM library

Indirect capital costs includes the sales tax, land cost, EPC and owner cost. EPC and owner costs were kept as 11% of the total direct cost. Land cost was taken as $ 10000 per acer which is the SAM default value.

Operation and maintenance costs include the expenditures on equipment maintenance, their replacements and services that occur once the plant is installed. SAM provides the ways to enter these costs as fixed annual, fixed by capacity and variable by generation. Fixed cost by nameplate capacity was taken as 66 $/kWh-yr and variable cost by generation was taken as 4 $/MWh. Both of the above values were the default values in SAM software. These default values set in the software are the cost values obtained from the CSP plants running in United States. No escalation rate was imposed on the above operation and maintenance cost values in this simulation.

4.9 System Performance Degradation

The lifetime input allows the user to model a yearly decline in the power output of the plant due to aging of equipment over time. The degradation rate is used by the software to calculate the annual energy output in second year of operation and later. 0.5% of annual degradation rate was assumed for the simulation.

4.10 Financial Parameters

In order to simulate the financial performance of the CSP plant under study, a solution mode has to be specified at the beginning. There are two options available in the financial parameters page and among them the first is to specify an IRR target. In this

option software calculates PPA price based on the specified value of IRR and the year of achievement. Second option is to specify PPA price and the software calculates project IRR. PPA price is the price that has to be negotiated as a part of power purchase agreement. The PPA price mode was selected for this analysis. The PPA price used was 0.1148 $/kWh. This value was calculated considering the purchasing price of Rs.18.37 in Sri Lanka for solar PV under the project "Sooryabala Sangramaya" and converting it to US dollars at an exchange rate of Rs.160.00 per 1 US dollar.

Analysis period was considered as 30 years. The discount rate used for the analysis was 15%. In this analysis uniform dispatch was considered where all PPA price multipliers were set to 1 throughout the day and for week days and weekends in time of delivery factors page.

4.11 PPA price for positive NPV

It was noticed by the initial simulation results for the CSP plant under study, the NPV is negative. The capital cost of the project cannot be decreased but the revenue can be increased by selling power at higher price. Using the parametric simulation facility in SAM software, an analysis was performed in order to find out the PPA price which results a positive value for NPV which attract the investors on the project. PPA price was varied from 0.1 $/kWh to 0.3 $/kWh in steps of 0.01 $/kWh and the financial performance indices were obtained. Present values of capital costs with the optimum TES size, SM and the best SCA type were used for this simulation.

4.12 Future cost of proposed CSP plant

In the literature review it has been found that the capital cost of CSP projects are reducing at a rate of 30% in every five years' time [17]. Considering this fact the financial parameters LCOE, IRR and NPV were calculated in order to check whether the project is feasible in future. The financial parameters of the project at present, and after every five years time for twenty years period in future were calculated considering the drop rate in the capital cost. In this study LCOE, IRR and NPV were calculated for the present capital cost and for the capital costs after every five years time for another twenty years period considering the rate of drop in the capital cost.

The present capital cost was reduced by 30% for each five year period for each cost category such as cost of solar field, power block, thermal energy storage, site preparation, etc., and the values were fed in to the SAM software in order to get the total capital cost of the project.

Using the capital cost values calculated for future, two studies were performed. For the first study two scenarios were considered. One with optimum size of thermal energy storage and the other without a thermal storage. The total capital cost and energy generation was obtained using the SAM software for the two scenarios. Considering the rate of reduction in capital cost the present values and future values of financial parameters for every five years were calculated and compared. The same study was extended further and analysed the financial performance indices for the variations in the rate of capital cost reduction. In addition to the main analysis of 30% cost reduction rate, NPV and LCOE values were obtained for the cost reduction rates of 25% and 35% as well for every five year time periods, considering the optimum storage size of 7 hours and without storage.

The second analysis was done to obtain the financial performance parameters with different TES sizes at different time levels of starting the project. Capital cost values were found for storage sizes of 0 hours to 10 hours at intervals of 1 hour at present cost and for future cost in 5 year intervals. The financial performance indices were calculated using the capital cost values in order to study the financial feasibility of the project in future.

4.13 Sensitivity analysis for discount rate

The discount rate used for the simulation in this study is 15% by considering the real discount rate and inflation rate. However the discount rate for a power generation projects may vary time to time according to the economic condition in the country. Therefore a sensitivity analysis has been performed considering the discount rates of 10% and 20% and compared the financial performance of the plant for present and future cost values.

4.14 Performance analysis for variation in DNI data

When using SAM to predict the power output of CSP plant, uncertainty of DNI data in the library could be one of the main sources of uncertainty in the simulation results. In this simulation, the performance is predicted for future using historical weather data. The available DNI values are satellite data and they might vary at the ground level. Because of this uncertainty of solar radiation data, simulations were performed for 10 MWe parabolic trough CSP plant considering +5% and -5% of DNI data. +5% and -5% of hourly direct solar radiation was calculated using the available data in SAM library for Hambanthota and fed in to the software to obtain the technical and financial performance.

4.15 Performance of 25 MWe and 50 MWe plants

Parabolic trough CSP plants of capacity 25 MWe and 50 MWe were also simulated to study how the plant performs technically and financially at the higher capacities. Optimum values of solar multiple and TES full load hours found for the 10 MWe plant in the initial study were used for this analysis as well. Type of HTF and SCA used in here were also the best ones for the 10 MWe plant. SEGS 30MWe power block reference system used for 25 MWe plant and SEGS 80 MWe power block reference system was used for 50 MWe plant. TES dispatch control, system costs, financial performance parameters, degradation and time of delivery factors were kept at same values as in the previous simulations.

5 RESULTS

5.1 Solar Multiple and Thermal Energy Storage

Parametric simulations were performed in order to identify the best combination of solar multiple and the size of TES. LCOE was used as the performance indicator in this analysis. Table 5.1 shows the optimum values of Solar Multiple for different sizes of TES from 0 hours to 10 hours which minimizes LCOE. The results clearly indicates that the size of solar field area has to be increased with the size of TES. LCOE is 29.07 cents/kWh for a parabolic trough CSP without storage and the value of LCOE decreases with the size of TES. This is due to the increase in annual energy output with the increase of TES size and solar multiple. The minimum value for LCOE is 27.60 cents/kWh for the combination of storage size 7 hours and solar multiple 3.5. IRR is 3.60% for this combination. When the size of thermal storage is above 7 hours the solar multiple should be 4 to get the minimum LCOE. Though the annual energy output increases with TES size and solar multiple, the LCOE decreases when the storage size greater than 7 hours. NPV is negative for all combinations of TES capacities and solar multiples.

Table 5.1: Simulation results for selecting TES size and Solar Multiple

TES size (hours)	Solar Multiple	Annual energy (GWh)	LCOE (cents/kWh)	IRR (%)	NPV ($)
0	2.0	24.76	29.07	2.38	-27739200
1	2.5	30.45	28.02	3.02	-32075800
2	2.5	32.08	27.73	3.19	-33188800
3	3.0	36.77	27.80	3.33	-38224600
4	3.0	38.31	27.63	3.42	-39404900
5	3.0	39.52	27.70	3.43	-40816700
6	3.5	44.42	27.64	3.56	-45704700
7	3.5	45.80	27.60	3.60	-46999500
8	4.0	50.55	27.63	3.67	-51992600
9	4.0	51.51	27.82	3.62	-53582700
10	4.0	52.41	28.03	3.57	-55216800

Figure 5.1 is a graphical representation of variation of LCOE with solar multiple under different capacities of thermal energy storage.

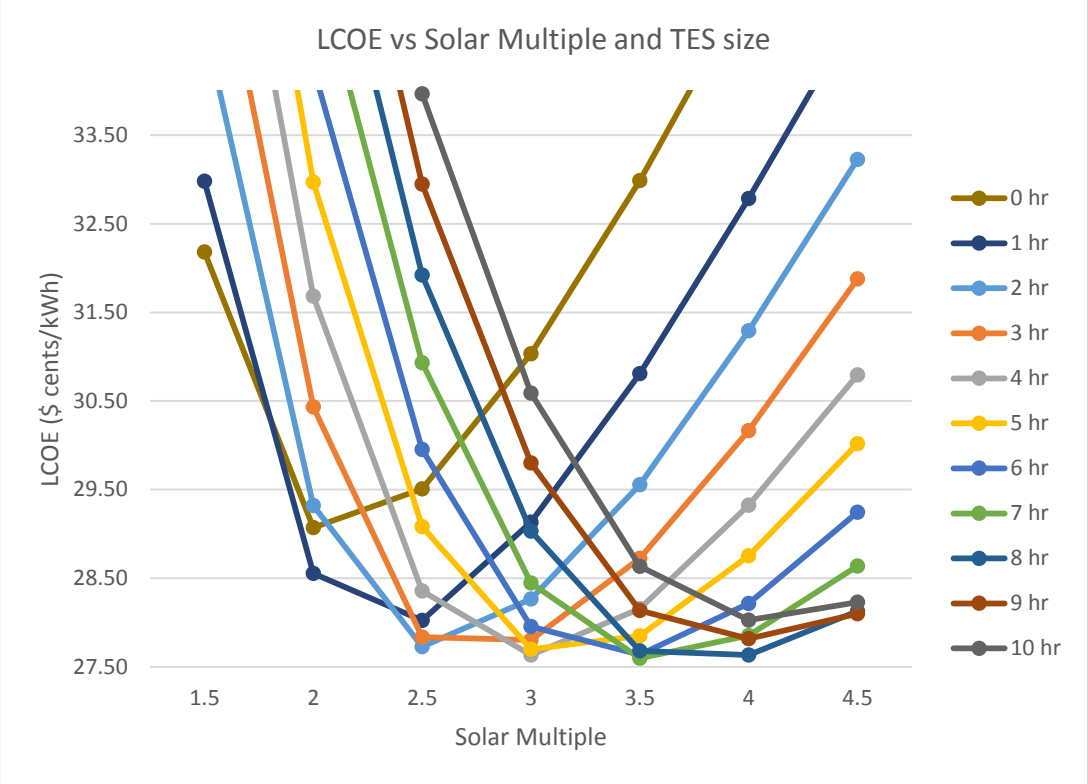

Figure 5.1: Variation of LCOE with Solar Multiple and TES size

5.2 Heat Transfer Fluid

Simulation results for the 10 MWe plant with different types of heat transfer fluids are presented graphically. Comparison of annual energy generation and capacity factor with different types of heat transfer fluids are shown in figure 5.2 and figure 5.3 respectively. The highest annual energy generation of 45.8 GWh in the first year of operation is produced when using Therminol 66 as the heat transfer fluid and the highest capacity factor of 52.8% is also obtained with the same fluid. Caloria HT 43 produces 44.6 GWh with a capacity factor of 51.4% in the first year of operation, which is the second best option as a HTF.

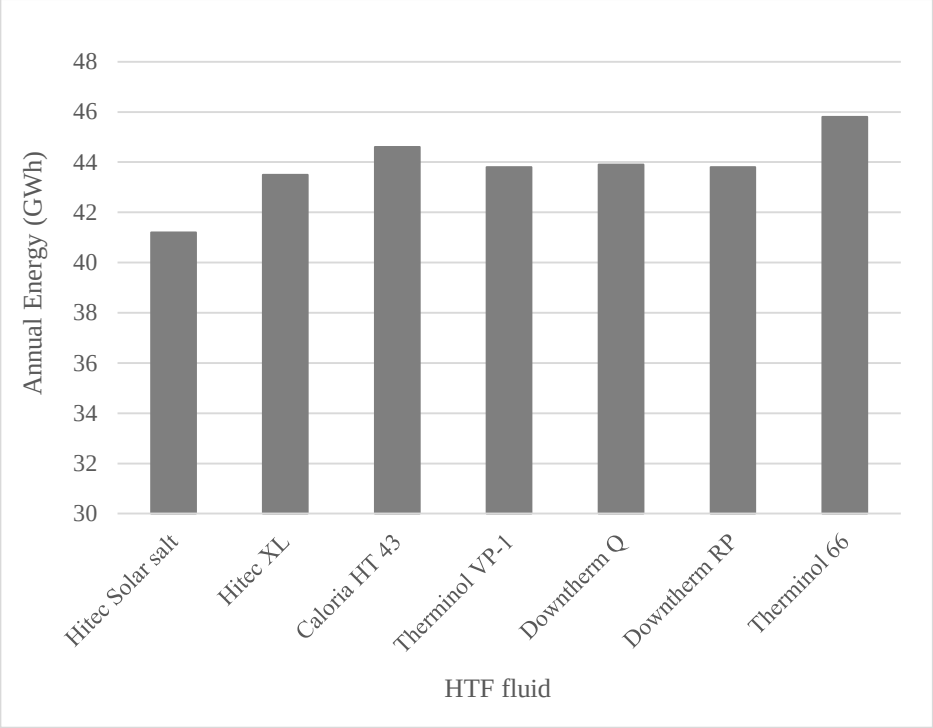

Figure 5.2: Annual energy output with HTF types

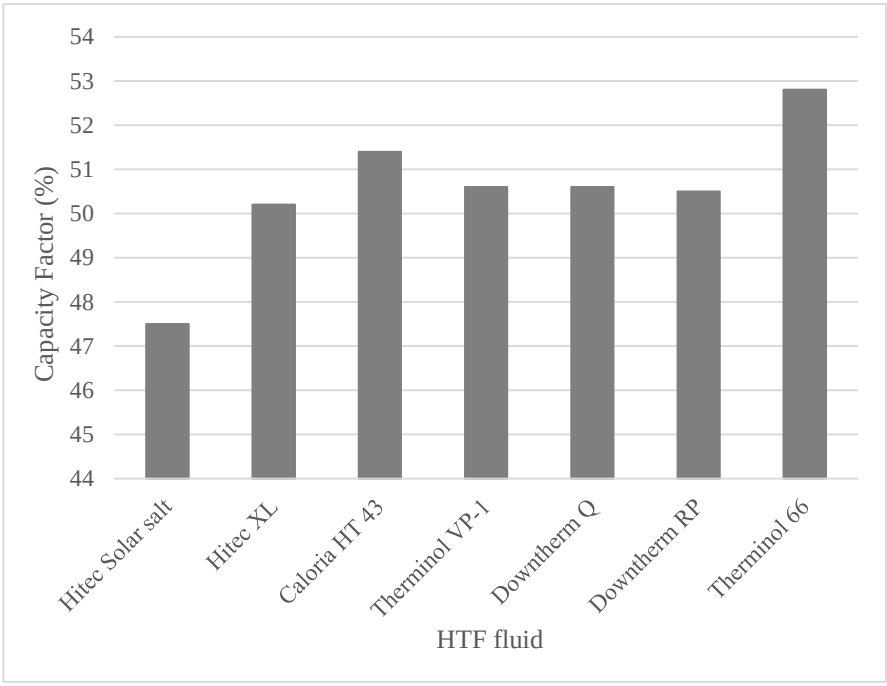

Figure 5.3: Capacity factor with HTF types

The plant under the study shows its best financial performance when using Therminol 66 as the heat transfer fluid. Highest IRR and lowest LCOE are shown with this fluid as shown in figure 5.4 and figure 5.5 respectively.

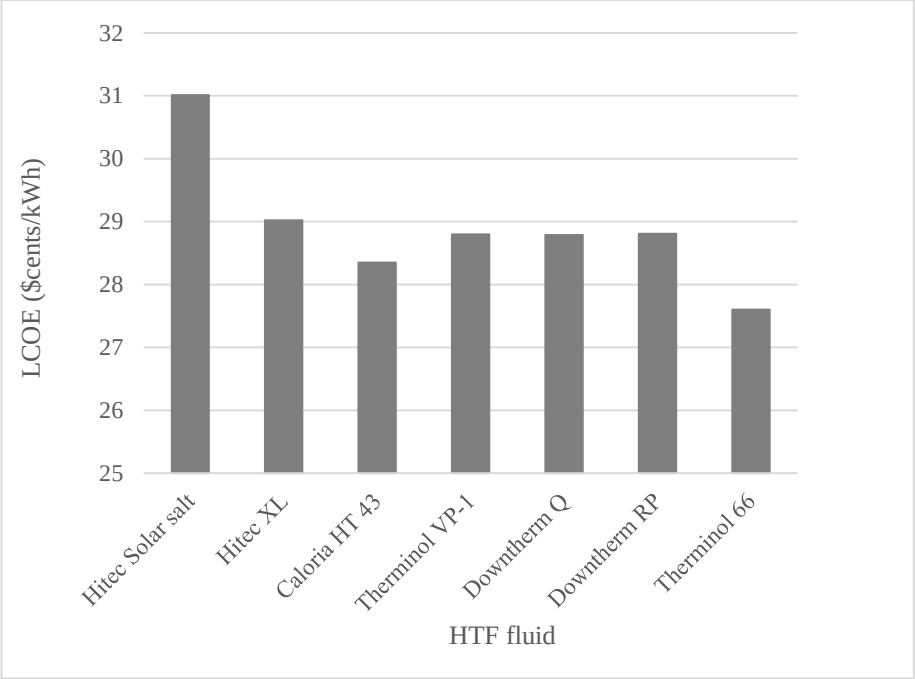

Figure 5.4: LCOE with HTF types

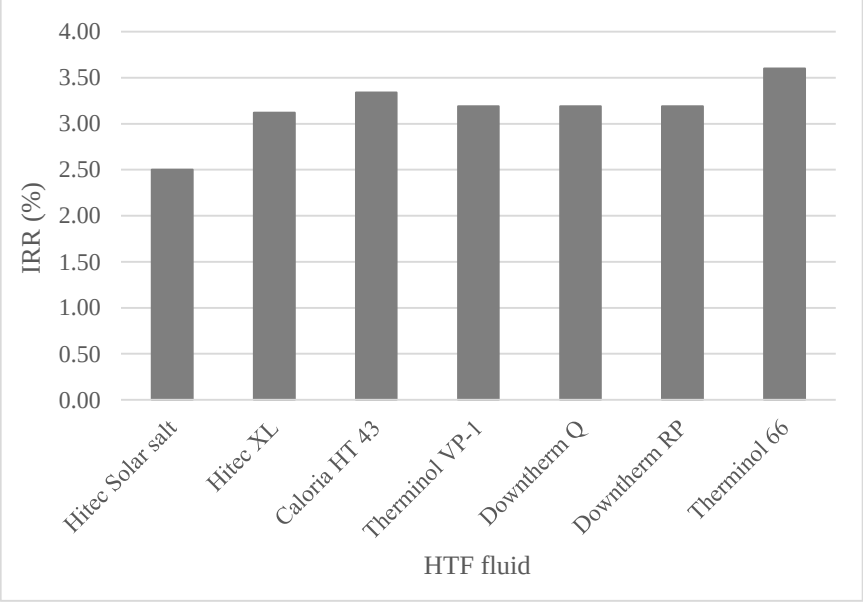

Figure 5.5: IRR with HTF types

5.3 Selection of SCA

Results of the SAM simulation of the plant with different types of solar collector assemblies (SCA) are shown in this section. Figure 5.6 shows that Solargenix SGX-1 SCA type can generate highest annual energy of 45.8 GWh in the first year of operation. Albiasa Trough, Luz LS-2 and Luz LS-3 are the SCAs that can be considered as the second best options which can produce 45.5 GWh in the first year.

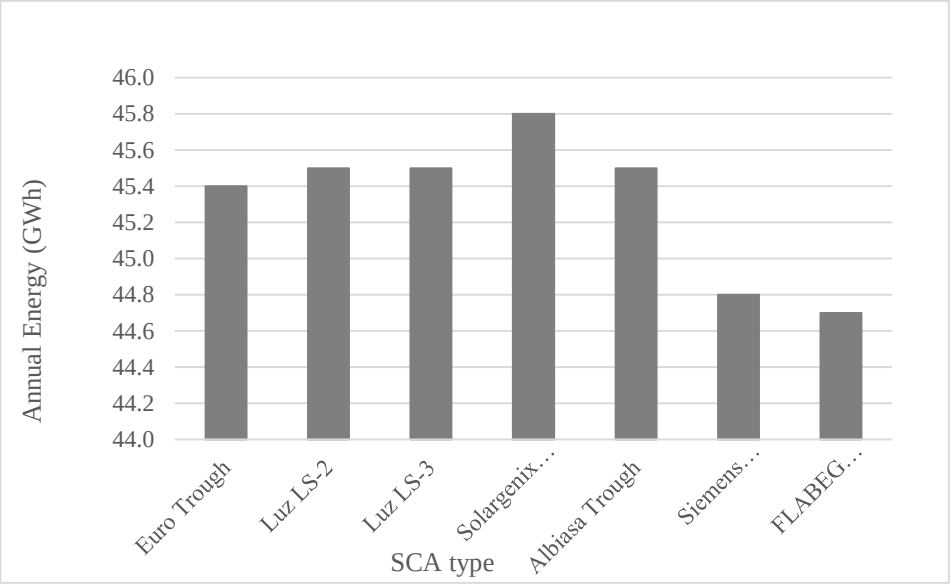

Figure 5.6: Annual Energy output with SCA types

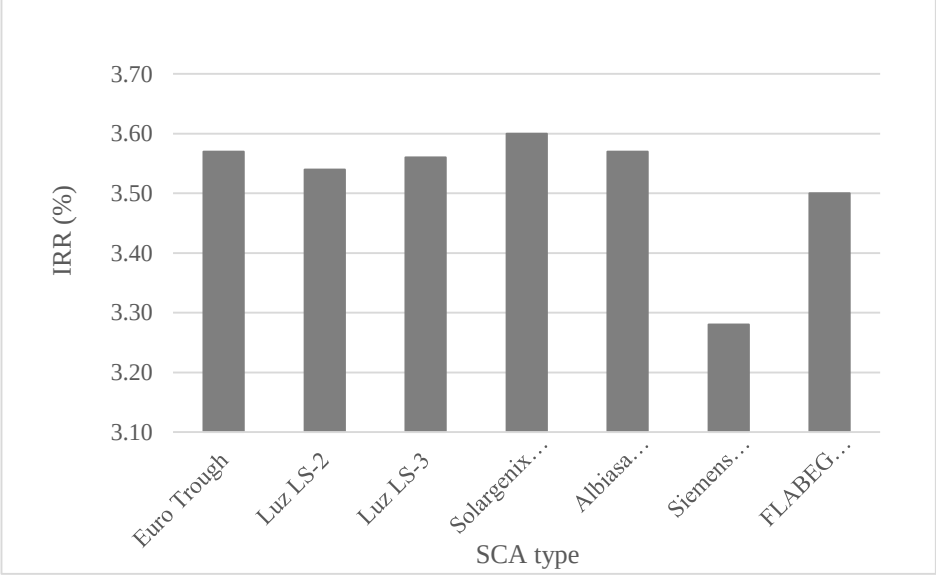

Figure 5.7: IRR with SCA types

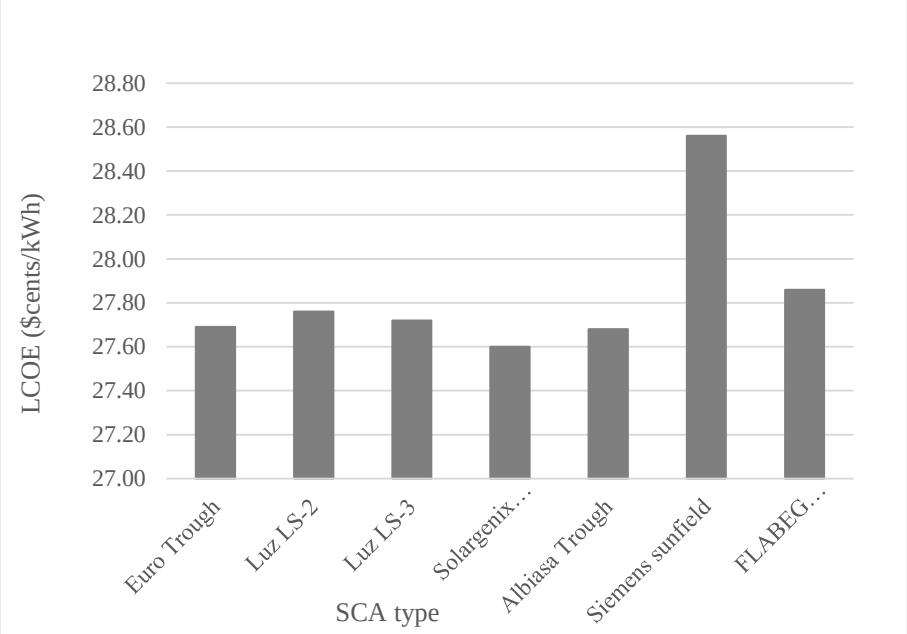

Figure 5.8: LCOE with SCA types

When considering the financial performance parameters, the highest figure of IRR is resulted when using Solargenix SGX-1 as the SCA as indicated in figure 5.7. Figure 5.8 displays the different values of LCOE with different types of SCAs. The LCOE become lowest for the collector assembly type of Solagenix SGX-1, and it is slightly high with Albiasa Trough and Euro Trough. LCOE is significantly high for the SCA type Siemens sunfield.

5.4 Performance of 10 MWe plant

5.4.1 Technical Performance

The calculated values during the simulation related to area of the solar field and number of SCAs are presented in table 5.2. Land area for solar field is 108 acers and total land area required for the 10 MWe plant is 151 acers.

According to the calculations by the software, the thermal energy required by the power block to generate the gross electric output which is known as the design turbine thermal input is 29.3 MWt. The maximum and minimum thermal energy delivered to the power block by solar field, TES or both are 33.6 MWt and 8.7 MWt respectively. Maximum thermal energy storage is 205.3 MWht. Maximum power delivered to

storage is 118 MWt and maximum power delivered from storage to power block is 34.2 MWt. Total parasitic energy consumption at design point is 2.7 MWe.

Table 5.2: Results from solar field page

Parameter	Value
Aperture reflective area (m^2)	146,498
Aperture reflective area SM=1 (m^2)	41,633
Exact no. of SCAs (for SM=1)	88
Aperture area per SCA (m^2)	470
Solar field land area (acers)	108
Total land area – multiplying factor 1.4 (acers)	151
Solar field piping heat losses (W/m^2)	3.7

5.4.2 Financial Performance

The total directed capital cost for the plant under study with the present cost values is $ 66,226,432. The resulted direct capital cost values under different sections of the plant are tabulated in table 5.3.

Table 5.3: Direct capital costs for 10 MWe plant

Cost category	Value
Site Improvements ($)	3,808,959
Solar Field ($)	21,974,768
HTF system ($)	8,789,907
Thermal Storage ($)	13,350,226
Power Plant ($)	12,650,000
Balance of Plant ($)	1,320,000
Contingency ($)	4,332,570

The total indirect capital cost for the plant is $ 8,797,187 and the distribution of it under different cost categories is listed in table 5.4. The total installed cost of the plant

is $ 75,023,616 and the total estimated installed cost per net capacity is $ 7,578 per kilo Watt.

Table 5.4: Indirect costs of the plant

Parameter	Value
Land cost ($)	1,512,279
EPC and Owner cost ($)	7,284,907

The annual energy generated by the 10 MWe parabolic trough CSP plant at Hambanthota for the first year is 45,800,228 kWh. The capacity factor of the plant for the first year is 52.8%. Values of LCOE, NPV,IRR are available in the results summary provided by the SAM. This summary results sheet is shown in table 5.5.

Table 5.5: Summary of results for 10 MWe plant

Metric	Value
Annual energy (year 1)	45,800,228 kWh
Capacity factor (year 1)	52.8%
PPA price (year 1)	11.48 ¢/kWh
PPA price escalation	0.00 %/year
Levelized PPA price (nominal)	11.48 ¢/kWh
Levelized PPA price (real)	11.48 ¢/kWh
Levelized COE (nominal)	27.60 ¢/kWh
Levelized COE (real)	27.60 ¢/kWh
Net present value	$-46,999,488
Internal rate of return (IRR)	3.60 %
Year IRR is achieved	30
IRR at end of project	3.60 %
Net capital cost	$75,023,616
Equity	$75,023,616
Size of debt	$0
Minimum DSCR	Inf

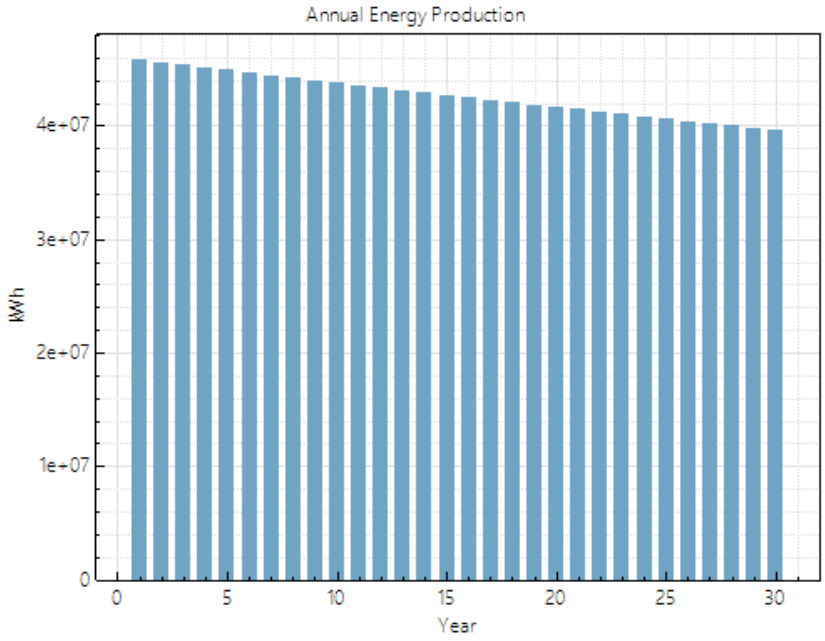

Figure 5.9: Annual energy production with number of years

The expected annual energy output for the 30 year period of operation is shown in the figure 5.9. Since a performance degradation rate of 0.5% per year is considered in the simulation the output is expected to be decrease at a constant rate during the period of operation. In the first year of plant operation, the monthly energy output is shown in figure 5.10.

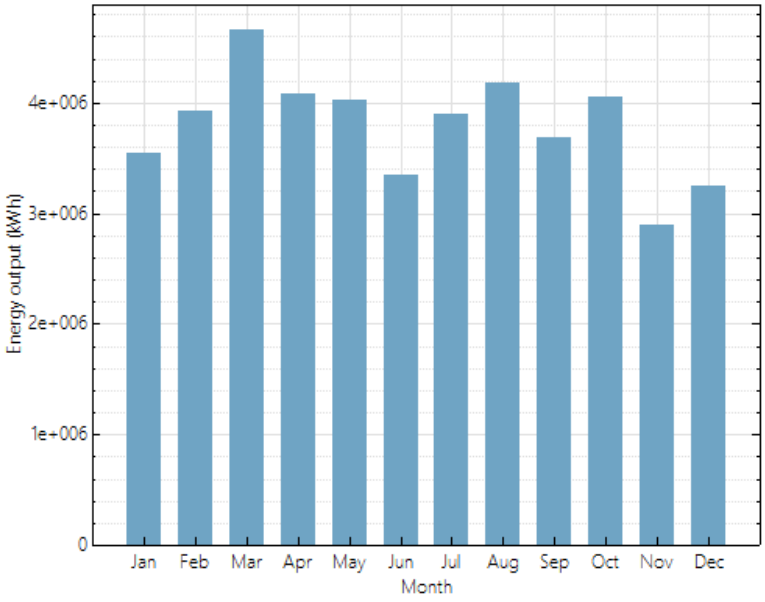

Figure 5.10: Monthly first year energy generation

5.5 Energy profiles of 10 MWe plant

Figure 5.11 shows how the thermal energy incident on SCAs of the solar field and thermal power absorbed by HCEs in the solar field varies with time in each month. It includes the annual profiles as well. Figure 5.12 shows how the TES performs in each month and in the whole year. It indicates how thermal energy is received to TES and how thermal energy is delivered from storage to the power block with time. Figure 5.13 shows monthly net electrical power output from the plant.

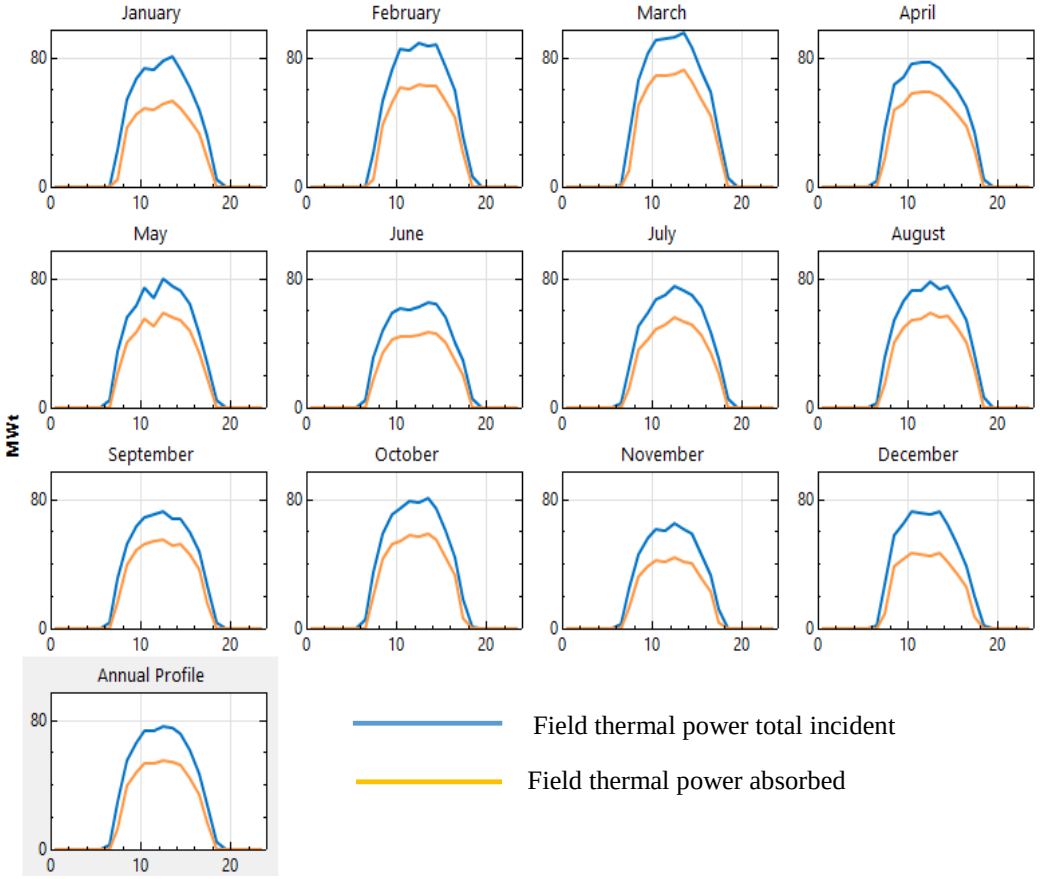

Figure 5.11: Monthly and annual thermal power incident and absorbed

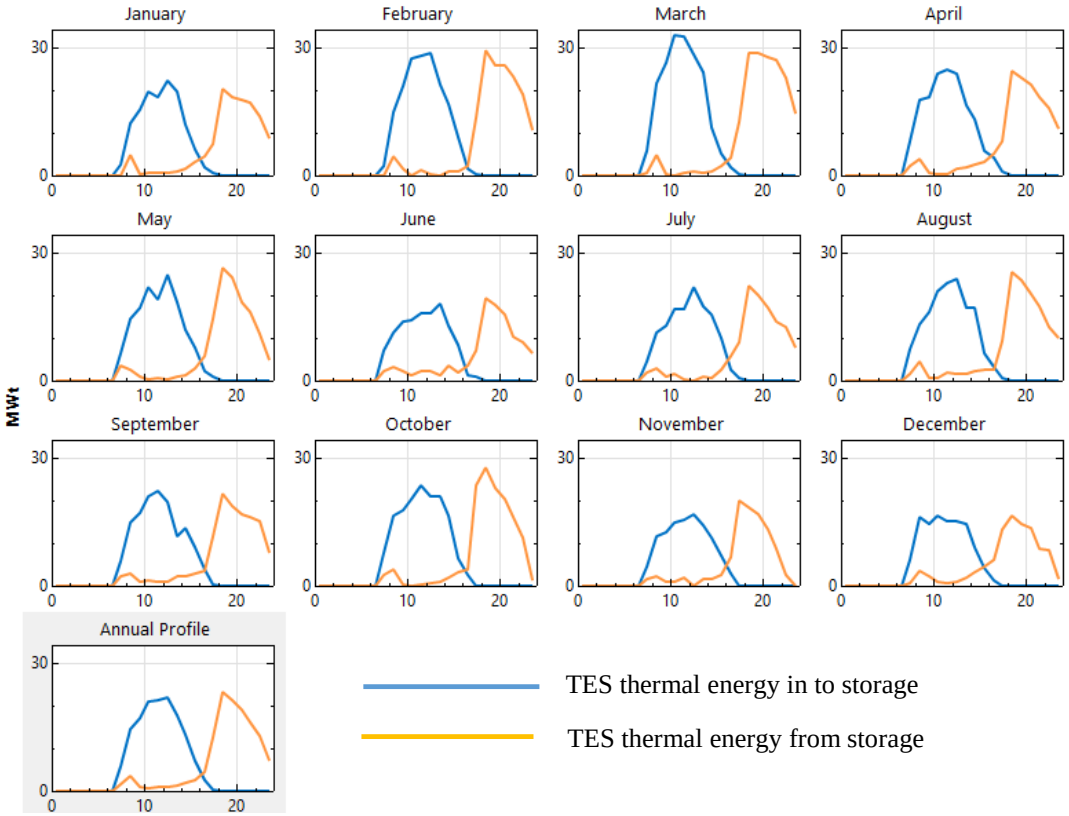

Figure 5.12: Monthly and annual TES performance

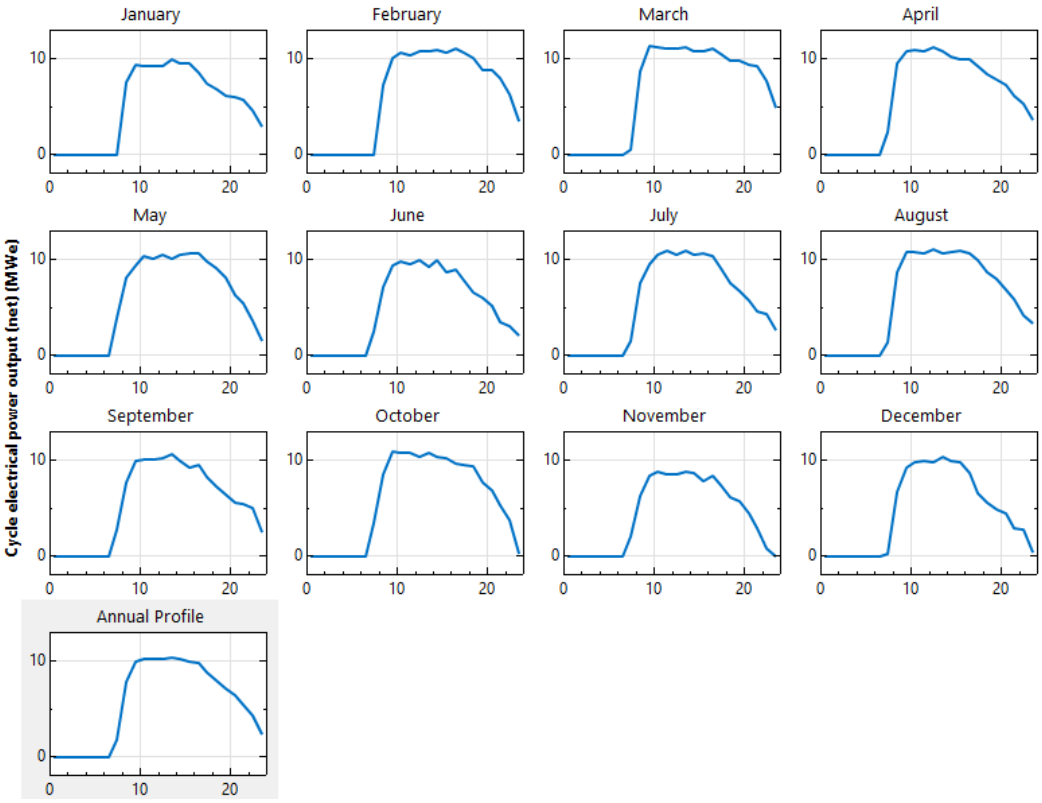

Figure 5.13: Monthly and annual electrical power output of the plant

5.6 PPA price for positive NPV

It has been noticed that with the present PPA price the NPV is negative for the 10 MWe parabolic trough CSP plant under study. Hence the project does not seem to be attractive for the investors. Therefore set of simulations were performed in order to identify the price which makes the NPV positive with the present cost values of the plant. Results are shown in table 5.6. For NPV to be positive the PPA price is 0.28 $/kWh (Rs.44.80/kWh, with the exchange rate of $1 = Rs. 160). That is more than the twice of present PPA price for solar generated electricity.

Table 5.6: Increase in NPV with PPA price

PPA price (Rs/kWh)	PPA price ($/kWh)	IRR (%)	NPV ($)
16.00	0.10	2.24	-51725100
17.60	0.11	3.15	-48808600
19.20	0.12	4.01	-45892200
20.80	0.13	4.84	-42975700
22.40	0.14	5.63	-40059300
24.00	0.15	6.39	-37142800
25.60	0.16	7.14	-34226400
27.20	0.17	7.86	-31309900
28.80	0.18	8.57	-28393400
30.40	0.19	9.27	-25477000
32.00	0.20	9.95	-22560500
33.60	0.21	10.63	-19644100
35.20	0.22	11.29	-16727600
36.80	0.23	11.95	-13811200
38.40	0.24	12.61	-10894700
40.00	0.25	13.25	-7978250
41.60	0.26	13.89	-5061800
43.20	0.27	14.53	-2145330
44.80	0.28	15.17	771121

5.7 Analysis of different scenarios

The direct radiation data used in the study were taken form SWERA programme. The DNI data provided here are measured from satellites. Therefore, there may be variations in this data at the ground level. The results of the simulations performed for the 10 MWe plant considering 5% more direct radiation and 5% less direct radiation are compared in table 5.7.

Table 5.7: Plant performance at ± 5% DNI

Parameter	Value		
	-5% DNI	**DNI**	**+5% DNI**
Annual energy (GWh)	44.3	45.8	47.1
Capacity factor (%)	51.1	52.8	54.3
LCOE (¢/kWh)	28.52	27.60	26.86
NPV ($)	-48,064,264	-46,999,488	-46,103,032
IRR (%)	3.28	3.60	3.87
Net capital cost ($)	75,023,616	75,023,616	75,023,616

5.8 Project feasibility analysis for future cost

Considering the fact that the capital cost of CSP projects are having a decreasing trend at a rate of 30% in every five years time set, of the financial parameters were calculated for the project. In the analysis capital cost for the 10 MWe plant was calculated for the present cost values using the SAM software and capital costs for every five years for the plant were calculated considering the price drop rate of 30%. The results indicate the financial performance of the plant at present cost and after every five years time for twenty year period. Figure 5.14 to figure 5.16 shows the values of LCOE, IRR and NPV under two different scenarios of no storage and seven hours storage.

The LCOE of the project has a decreasing trend for both no storage and seven hours storage size with starting time of the project as illustrated in figure 5.14. With the present cost values the LCOE values for without storage and with optimum storage size are 0.29 $/kWh and 0.27 $/kWh respectively. If the project starts after 15 years time the LCOE is less than 0.11 $/kWh. This value is less than the present PPA price with seven hours storage.

The IRR has increasing trend with starting time and it is high for the plant with seven hours TES compared to a plant without storage. If the project is going to start after 15

years, with a TES capacity of seven hours, the rate of return will be greater than 15% which is greater than the discount rate considered in the analysis.

The results of the analysis illustrated in figure 5.16 indicates that the project is not an attractive one for the investors at present since the NPV is negative. If the project starts after 15 years, with the seven hours thermal storage the NPV become positive. But on the other hand NPV is negative for a project without energy storage even after 15 years.

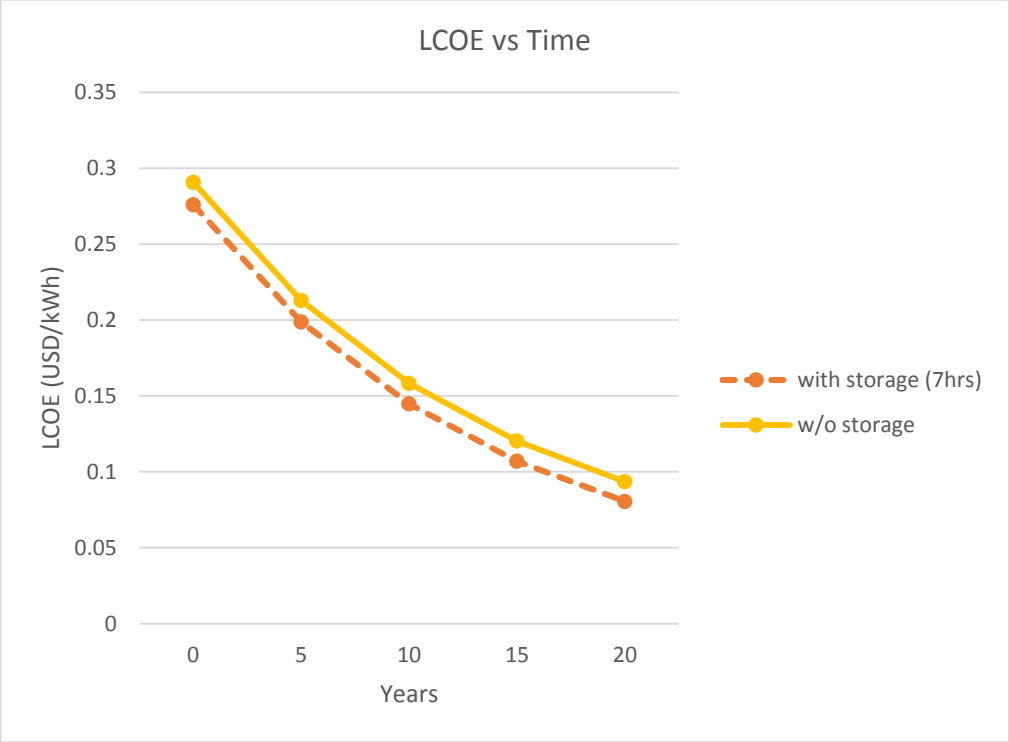

Figure 5.14: Variation of LCOE with project starting time

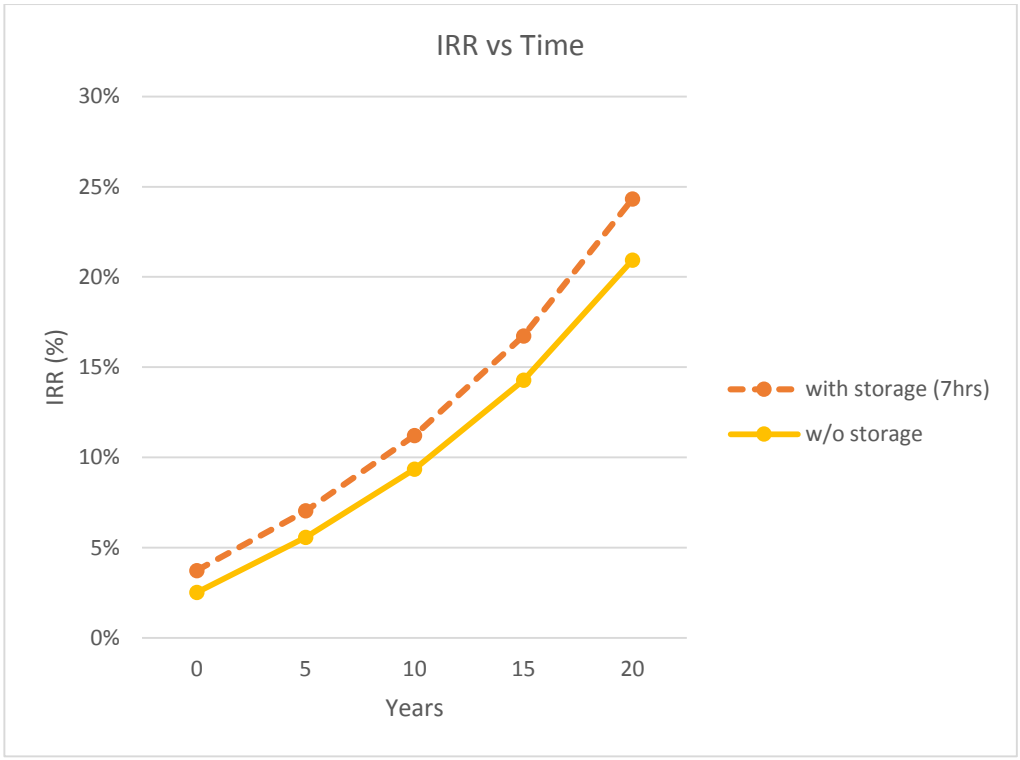

Figure 5.15: Variation of IRR with project starting time

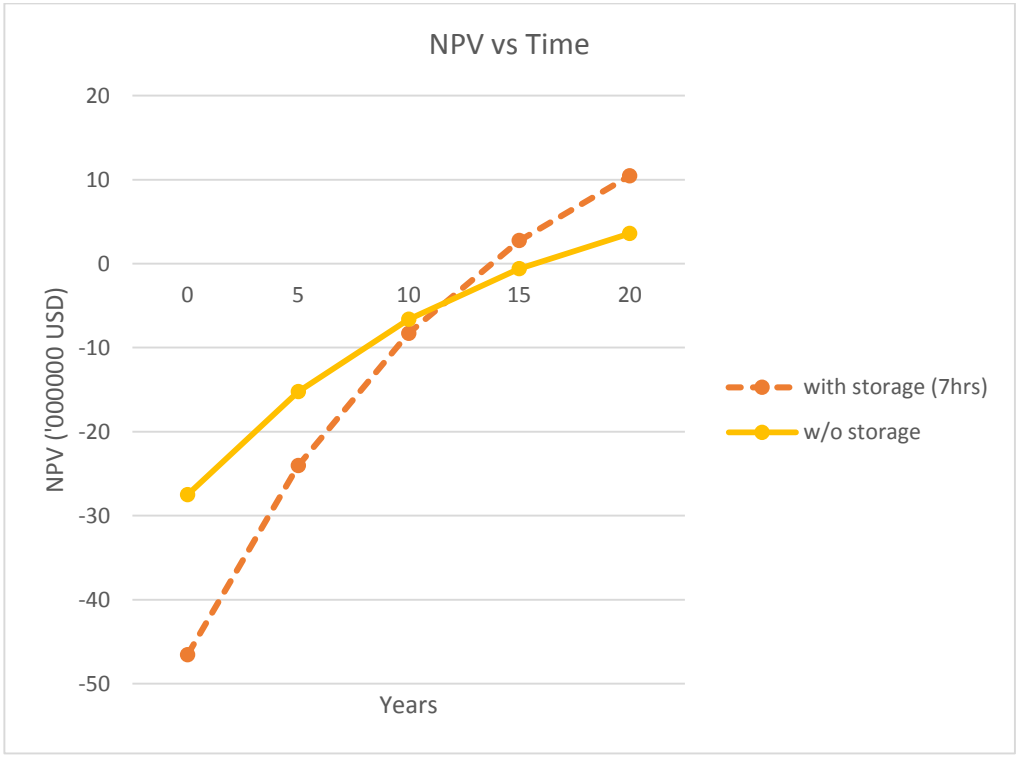

Figure 5.16: Variation of NPV with project starting time

More results of the study of the variation of financial performance indices are shown in the figure 5.17 to figure 5.19. Figure 5.17 shows the variation of LCOE with the size of thermal storage. It displays the variation of LCOE at different starting times of the project. At present, the unit cost of energy is above 0.27 $/kWh. From the results, it is noticed that the cost of energy will decrease in future due to the reduction in capital cost. The cost of energy is less than 0.12 $/kWh if the project starts after 15 years. The results also shows that the unit cost decreases with the storage size from 0 hours to 7 or 8 hours and it increases with storage size above 8 hours.

Figure 5.18 displays the variation of IRR with the TES size at different starting times of the project. At present the rate of return is below 4% and the results show that it increases with starting time. If the project start after 15 years the IRR is above 15% for the storage size above 2 hours. Another important fact noticed from the results is the IRR has increased with the storage size until 7 or 8 hours storage size and again shows a decreasing trend for storage sizes above 8 hours.

The variation of NPV of the project with storage size at different starting times shown in figure 5.19. With the present capital cost the NPV is negative and the negativity increases with the size of TES showing that the project is not attractive for the investors. If the project start after 15 years the NPV is positive when the size of storage is 2 hours or more. The highest NPV is noticed when the storage size is 8 hours after 15 years.

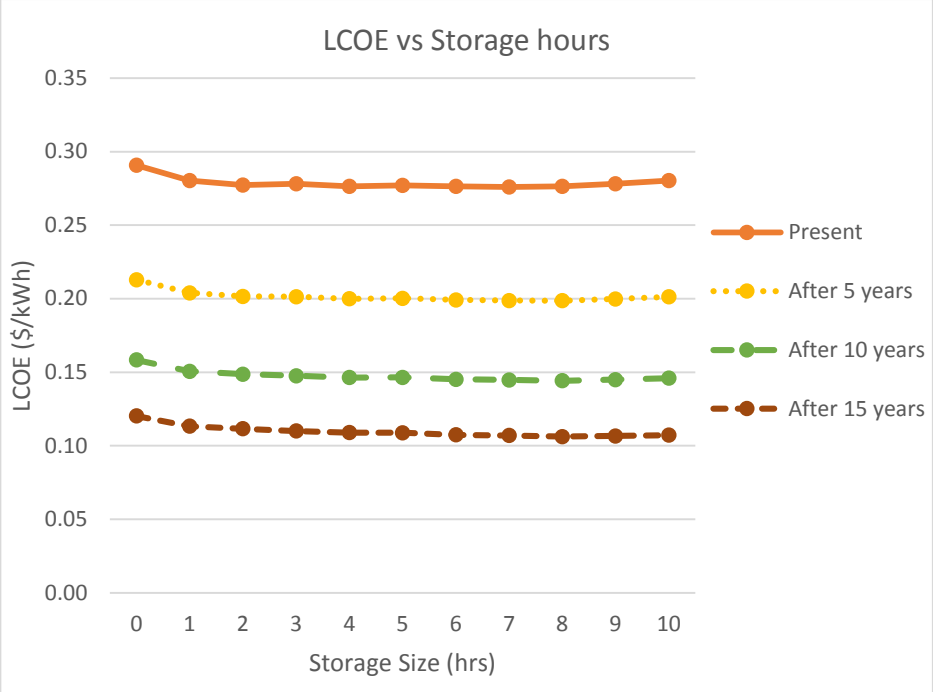

Figure 5.17: LCOE vs Storage size at different starting times

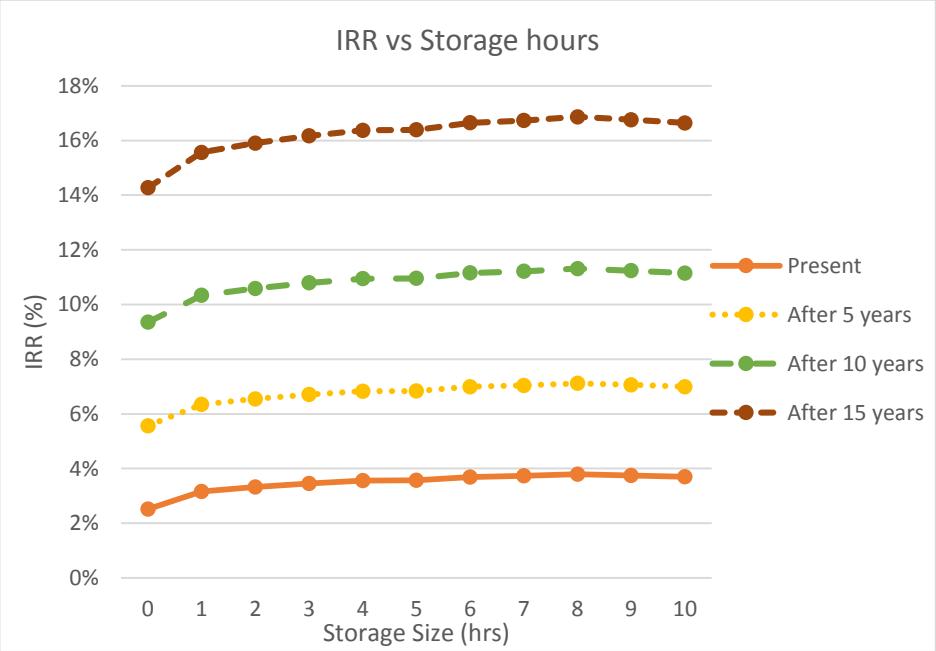

Figure 5.18: IRR vs Storage size at different starting times

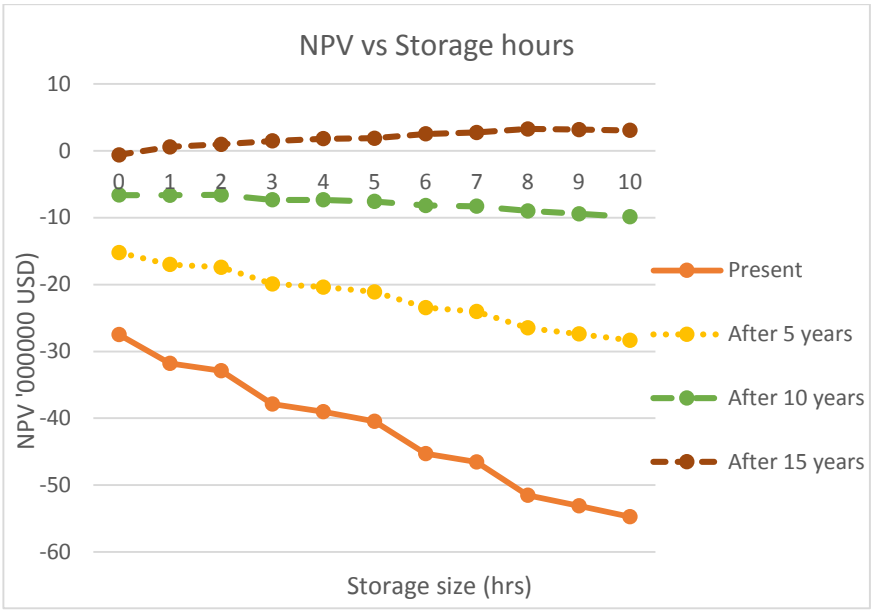

Figure 5.19: NPV vs Storage size at different starting times

Results of the analysis for capital cost reduction rates of 25% and 35% are compared with the financial performance parameters with the cost reduction rate of 30%. The variation of NPV and LCOE for present capital cost and future capital costs for every five years time for these cost reduction rates are expressed here. Figure 5.20 and figure 5.21 shows the results for 10 MWe plant with 7 hours thermal energy storage . Figure 5.22 and figure 5.23 shows the same results for the 10 MWe plant without storage.

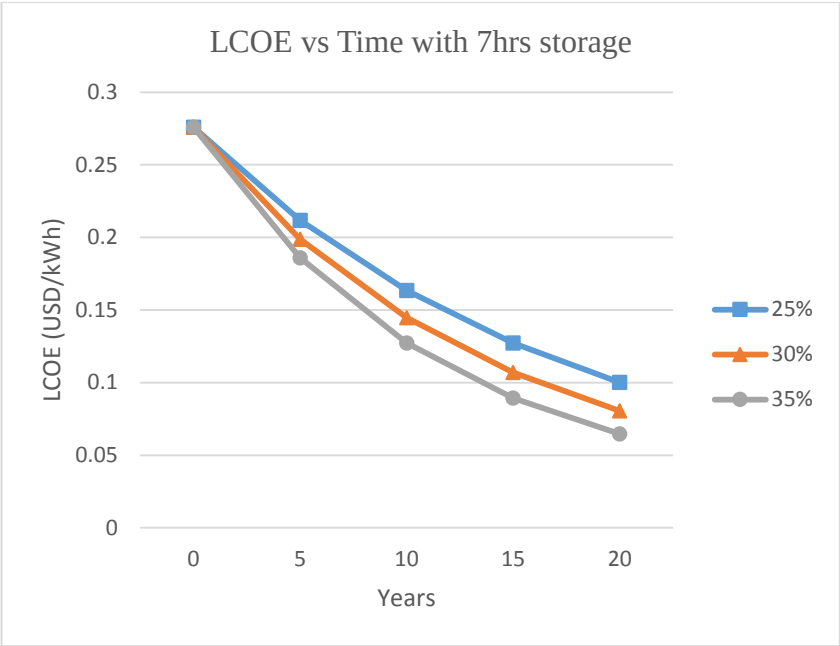

Figure 5.20: LCOE with project starting time at different cost reduction rates (with 7hrs storage)

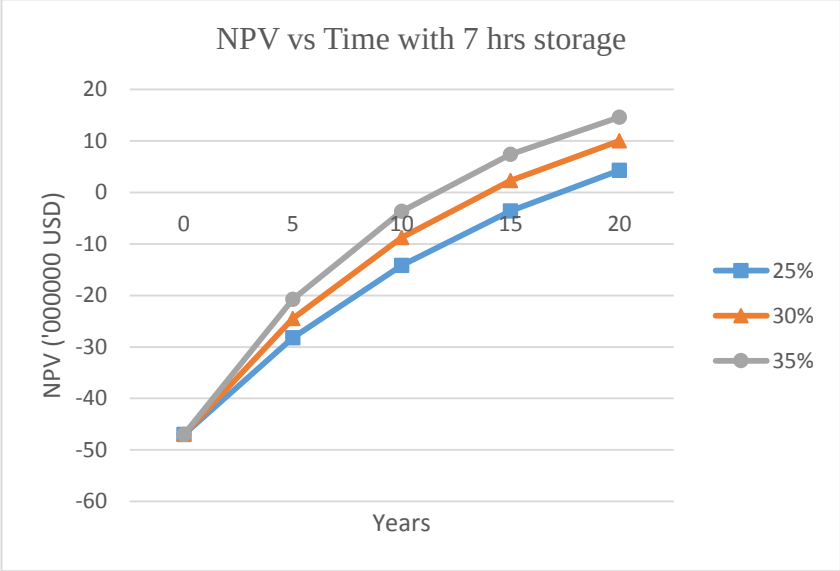

Figure 5.21: NPV with project starting time at different cost reduction rates (with 7hrs storage)

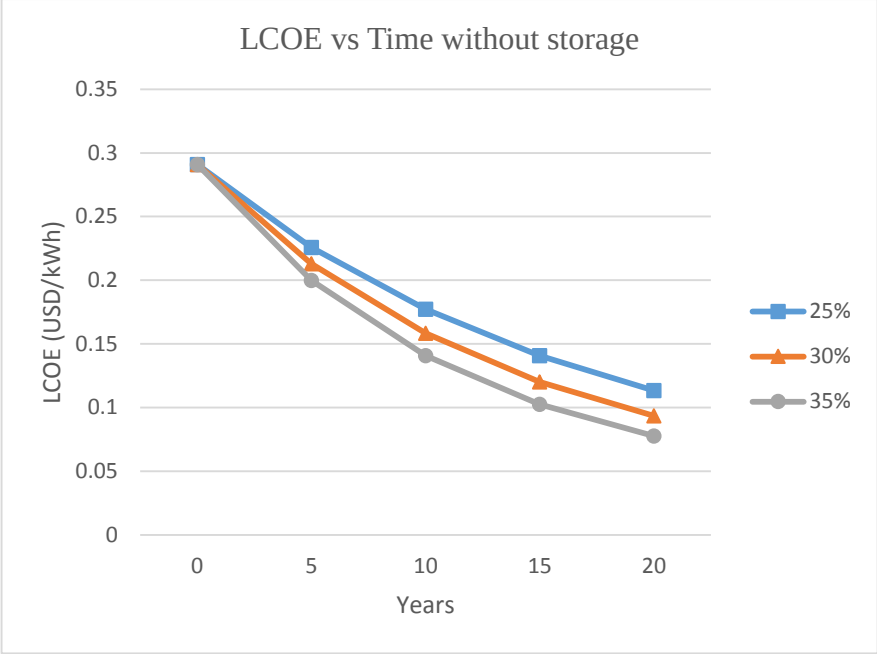

Figure 5.22: LCOE with project starting time at different cost reduction rates (without storage)

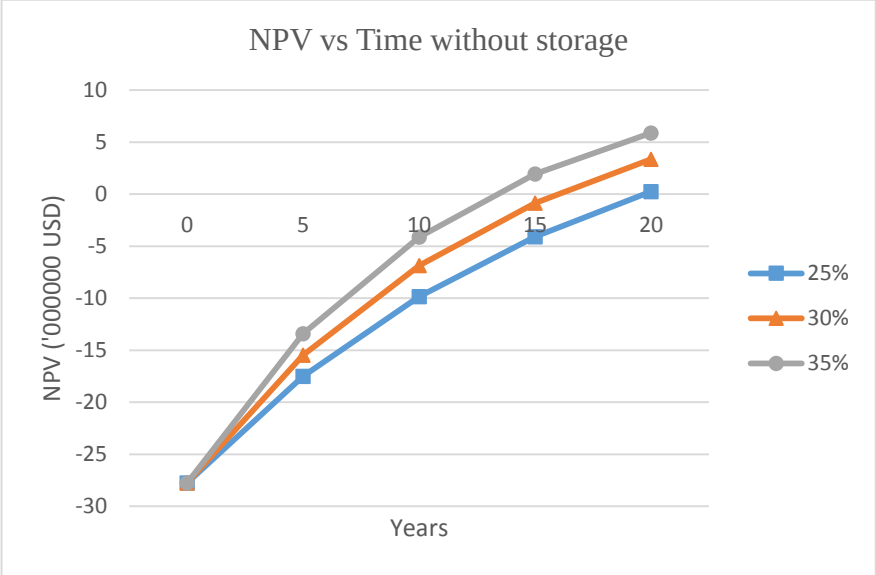

Figure 5.23: NPV with project starting time at different cost reduction rates (without storage)

5.9 Sensitivity analysis for discount rate

Results of the sensitivity analysis for discount rate are expressed in this section. NPV and LCOE for the present and future project cost values in five year time intervals were calculated for discount rates of 10%, 15% and 20% and then compared.

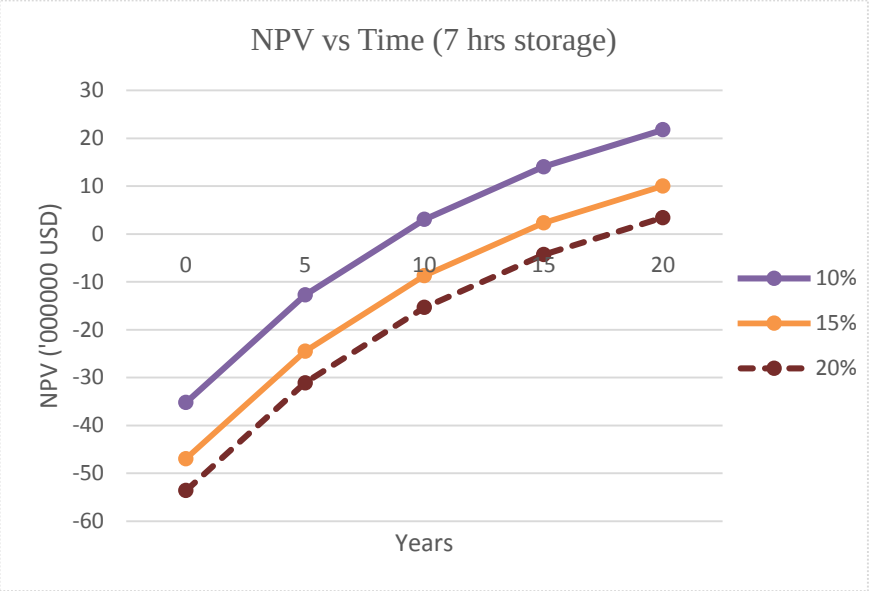

Figure 5.24: NPV with project starting time at different discount rates (with 7 hrs storage)

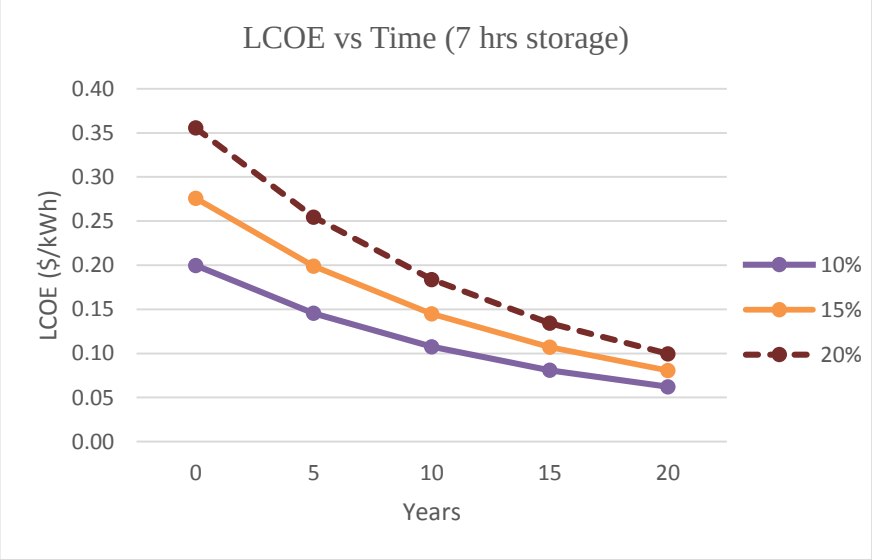

Figure 5.25: LCOE with project starting time at different discount rates (with 7 hrs storage)

Figure 5.24 shows the comparison of NPVs at different discount rates for the plant with 7 hours thermal energy storage. Figure 5.25 shows the comparison of LCOE for the plant with same storage size under the same discount rates.

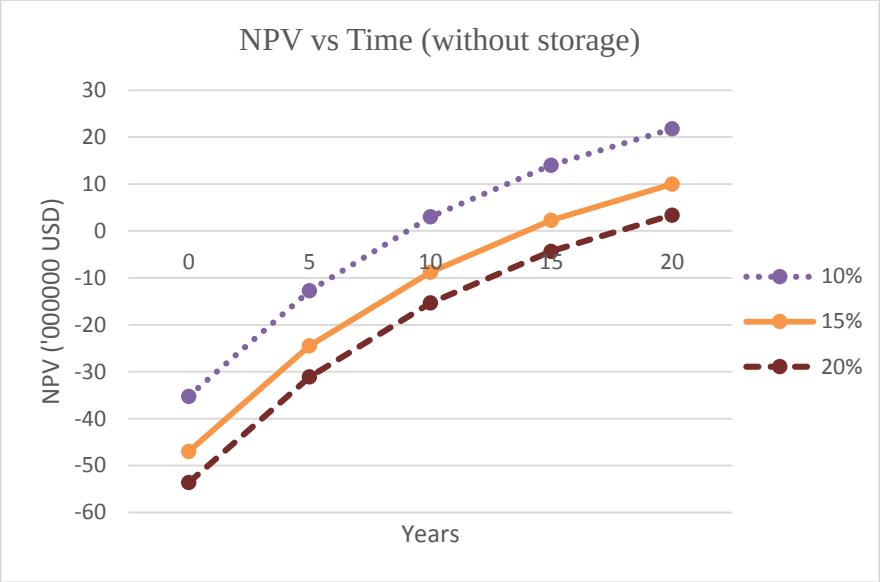

Figure 5.26: NPV with project starting time at different discount rates (without storage)

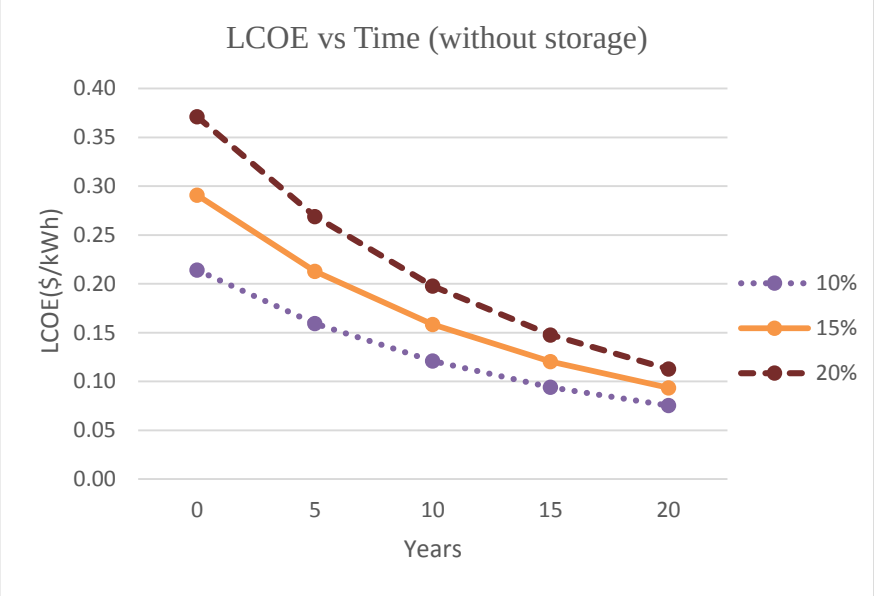

Figure 5.27: LCOE with project starting time at different discount rates (without storage)

Figure 5.26 and Figure 5.27 shows similar results for the plant without a thermal energy storage.

5.10 Performance of 25 MWe and 50 MWe plants

In addition to the 10 MWe plant under main study, 25 MWe and 50 MWe parabolic trough CSP plants were simulated and the results are displayed in the table 5.8. It is noticed that the LCOE for the plant become less with the increase in plant capacity. The LCOE is 0.2696 $/kWh for the 50 MWe plant. Simulation results shows that the plants of capacities 25 MWe and 50 MWe at Hambanthota can produce annual energy of 117 GWh and 235 GWh respectively. The net capital cost values for the plants of capacities 25 MWe and 50 MWe are 7,567 $/kWh and 7,512 $/kWh respectively.

Table 5.8: Comparison of 25 MWe and 50 MWe plants with 10 MWe plant

Parameter	**Value**		
	10 MWe	**25 MWe**	**50 MWe**
Annual energy (GWh)	45.8	116.9	234.9
Capacity factor (%)	52.8	53.3	53.7
LCOE (¢/kWh)	27.60	27.27	26.96
NPV ($)	-46,999,488	-117,535,056	-231,551,344
IRR (%)	3.60	3.72	3.82
Net capital cost ($/kW)	7,578	7,567	7,512
Land usage (acers)	151	382	758

6 DISCUSSION

The potential of electricity generation through concentrated solar thermal energy in Sri Lanka is not studied in detail. Purpose of this research is to fulfil that requirement and facilitate the policy makers in the country. As the first step, a literature survey was conducted in order to identify the most suitable technology and suitable location in the country. Parabolic trough concentrated solar thermal power plants are widely used and commercially well proven technology in the world. Since it is the most matured technology and most of the plants of the other technologies are still in their demonstration stage, it was decided to select parabolic trough technology. When considering the annual DNI levels of different locations in the country, only Hambanthota and Batticaloa had the direct radiation levels over 1600 kWh/m^2/year. Among them Hambantota was selected as the suitable location since it is the location with highest DNI. It was identified that the SAM software provided by NREL is a suitable software to simulate the performance of parabolic trough CSP plants.

In this study, a small scale parabolic trough CSP plant with capacity 10 MWe was simulated using the weather data at Hambanthota with SAM software. During the simulation it was noticed that the value of SM which defines the size of solar field and the size of TES are interdependent parameters. When the size of the solar field has increased the annual energy generation also has increased. But on the other hand with the solar field size, the capital cost has increased. By increasing the size of TES, the plant is able to store more thermal energy. But the size of the solar field should match with the size of TES in order to collect and supply enough thermal energy to the storage. High capacity TES also increases the capital investment. Results of the parametric simulations performed in order to find the optimum combination of SM and size of TES has shown that the best combination is SM of 3.5 and TES size of 7 hours of equivalent full load hours. This combination was the one which minimizes the LCOE.

Another aim of this study is to find out most economical heat transfer fluid for the plant. Simulation results shows that the highest energy generation can be obtained when using Therminol 66 as the heat transfer fluid as well as the media for thermal

energy storage. With Therminol 66 as the heat transfer fluid and TES media IRR is the highest and LCOE is lowest.

There are seven different types of pre designed solar collector assemblies available in the SAM library for empherical trough model. Out of them the SCA type Solargenix SGX-1 was found to be the most economical collector type when considering the simulation results. The plant can generate the highest annual energy with Solargenix SGX-1. Best financial performance was also seen with this type of SCA according to the results.

The results of the simulations performed for a 10 MWe parabolic trough plant with SM of 3.5 and TES capacity of 7 hours which uses Therminol 66 as its HTF can produce 45.8 GWh of energy in its first year of operation. The plant has a capacity factor of 52.8%. This is comparatively a high value when considering a plant of same capacity without TES. Simulation results have shown that the highest energy generation of this plant is in March and the lowest is in November. The energy output varies hourly with the variation of solar radiation and due to the weather condition of the region. The variation of energy output can be controlled significantly by the introduction of TES to the plant. The solar thermal energy incident profiles in figure 5.11 shows that the maximum of it is during the period of 12.00 hrs to 14.00 hrs. Figure 5.12 shows that the delivery of thermal energy from TES to the power block starts mainly during 16.00 hrs to 22.00 hrs. In order to cover the effect of cloud transitions, small percentage of energy supply from TES can be observed during the day time as well. The net electrical power output profile of the plant in figure 5.13 shows that the plant is in operation in its maximum capacity during 10.00 hrs to 16.00 hrs. Then the output gradually decreases and the plant generates energy till 22.00 hrs without solar energy incident since there is a supply of stored thermal energy from the TES. Further studies may require to match the energy output from the simulated CSP plant with the local grid requirement at Hambanthota.

When considering the financial performance parameters of the 10 MWe parabolic trough CSP plant, a negative value of $ -46,999,488 was resulted as NPV. The negative NPV value is an indication that the project is not attractive for the investors

at present cost. Project IRR was only 3.6% which is much less than the discount rate considered in the analysis. The LCOE was 0.276 $/kWh which is comparatively high value with the conventional methods of electricity generation. The total estimated installed cost per net capacity was 7,578 $/kW for the plant.

The study was extended to see the financial performance indices for the plant considering the reduction in cost in future. In the literature it was identified that the capital cost of the CSP technologies going to decrease by 30% in every five years' time with the technology development. Analysis were performed in order to obtain the financial performance of the 10 MWe plant under study obtain the LCOE, IRR and NPV in five year intervals for twenty years period considering the 30% cost reduction. According to the results of this analysis, it is found that the project will be financially feasible to operate after 15 years time with positive NPV. Further it is noticed that the NPV is positive with any size of TES after 15 years.

The results of the analysis for two scenarios of capital cost reduction rates of 25% and 35% shows that the NPV for the project is negative at 15 years with the rate 25% with thermal storage. It takes more than 15 years for NPV to be positive. But on the other hand for 30% and 35% cost reduction rates, the NPV become positive before 15 years. For the 10 MWe plant without storage the NPV become positive before 15 years when the cost reduction rate is 35%. For 25% cost reduction rate, it takes nearly 20 years to get positive NPV without a thermal storage. For the plant with 7 hours thermal energy storage, the LCOE is nearly 0.1 $/kWh for 25% cost reduction rate after 20 years. On the other hand LCOE is less than 0.1 $/kWh before 15 years for the cost reduction rate of 35%. For the plant without storage the levelized cost is just above 0.1 $/kWh with the cost reduction rate 35%.

For the case of the plant with 7 hours storage the NPV become positive before 10 years under 10% discount rate. On the other hand it takes more than 15 years for NPV to be positive under the discount rate of 20%. For the 15% discount rate, the value used for the main study, shows that the NPV become positive after 10 years. The NPV values for the plant without storage under the same discount rates shows almost similar results. For the project with 7 hours thermal energy storage, the LCOE is 0.20

$/kWh with 10% discount rate at present capital cost. If the discount rate is 20%, the LCOE is above 0.35 $/kWh with present capital cost. The LCOE will be less than the PPA price after 10 years with 10% discount rate. It takes 20 years to show the similar result with 20% discount rate.

Results of the simulations performed for 25 MWe and 50 MWe plants shows that the plants can generate 116.9 GWh and 234.9 GWh respectively during their first year of operation. The capacity factors are above 50% for both of the plants with 7 hours of TES and solar multiple 3.5. It is also noticed that the LCOE has reduced with the capacity of the plant. The LCOE values for the 25 MWe and 50 MWe plants are 27.27 $/kWh and 26.96 $/kWh respectively.

At present the country focused only on solar PV for power generation from solar energy. For utility scale solar PV system with one axis tracking, the capital cost is 1440 $/kWac [31] without energy storage. Cost of battery storage unit of a solar PV system is 500 $/kWhdc. Usually such a battery storage has to be replaced in every 10 years, hence for a plant of 30 years life time, three times the battery storage cost need to be considered. For a solar thermal plant the thermal energy storage cost is 65 $/kWht. Once this figure is converted to electric energy using the conversion ratios, it is 175 $/kWhe. The storage cost of the solar thermal plant is only around 12% of the battery storage cost of a solar PV plant. The total capital cost for the 10 MWe CSP plant with storage is 7,578 $/kW which is high compared to the solar PV plant without storage. By considering the cost of battery storage in solar PV and the drastic cost reduction rate in CSP technologies, the cost of CSP would be less than solar PV in future. A detailed analysis need to be done in order to compare the future cost of the two technologies.

7 CONCLUSION

Concentrated Solar Power (CSP) is a rapidly developing technology which is used for power generation. No proper analysis had been conducted yet to see the performance of this technology in the country. This research was conducted in order to select suitable CSP technology for the country and suitable location in the country, and also to study the performance of a small scale plant at the selected location. Parabolic trough was selected as the suitable technology considering the maturity of the technology and low cost. Hambanthota is the most suitable location since it has the highest Direct Normal Irradiation level of 1646 kWh/m^2/year. System Advisor Model (SAM) software developed by NREL was used to obtain the performance of 10 MWe parabolic trough CSP plant at Hambanthota.

Simulation results show that the plant can be operated at 52.8% capacity factor with a thermal energy storage (TES) while producing 45.8 GWh of energy in the first year under the optimum conditions of Solar Multiple 3.5 and TES size of 7 hours when Therminol 66 used as the heat transfer fluid and Solargenix SGX-1 used as the solar collector assembly. The results also suggest that the total cost of the CSP plant in this location is relatively high at the moment. Under these optimum conditions, the levelized cost of energy (LCOE) is 0.276 $/kWh. At present this is high compared to the power generation from coal and other renewable energy technologies operating in the country at present. The unit cost of electricity is 0.15 $/kWh for solar PV plant installed at Hambanthota. It was found that the net present value (NPV) is negative at present cost which may not be attractive for the investors. Further, the analysis conducted considering the capital cost reduction rate of 30% for CSP in every 5 years time has shown that the project will be financially feasible with positive NPV after 15 years period. The resulted LCOE at that time will be 0.11 $/kWh.

This analysis is performed as a feasibility study for implementing a CSP plant in the country and the study will provide a guideline for the policymakers. Detailed studies with a physical model may require in future before the implementation. Further it may require to match the power output of the plant with local grid requirement in Hambanthota

REFERENCES

[1] G. Brakmann, R. Aringhoff, M. Geyer and S. Teske. (2005, Sept.). Concentrated Solar Thermal Power – Now. Greenpeace, ESTIA. [Online]. Available: https://www.researchgate.net/publication/298944888_ Concentrated_ Solar_Thermal_Power_-_Now/download

[2] Renewables 2017: Global Status Report. (2017). [Online]. Available: http://www.ren21.net/wp-content/uploads/2017/06/17-8399_GSR_2017_Full _Report_0621_Opt.pdf

[3] 100% Electricity Generation through Renewable Energy by 2050: Assessment of Sri Lanka's Power Sector. (2017, August). [Online]. Available: https://www.adb.org/sites/default/files/publication/354591/sri-lanka-power-2050v2.pdf

[4] S. Kuravi, J. Trahan, D.Y. Goswami, M.M. Rahman and E.K. Stefanakos, "Thermal energy storage technologies and systems for concentrating solar power plants," *Progress in Energy and Combustion Science*, vol.39, no. 4, pp 285 - 319, August 2013.

[5] H. L. Zhang, J. Baeyens, J. Degreve and G. Caceres, "Concentrated solar power plants: Review and design methodology," *Renewable and Sustainable Energy Reviews*, vol. 22, pp. 466-481, June 2013.

[6] A. Krothapalli and B. Greska, "Concentrated solar thermal power", CSP Chapter 080310, Florida State University. [Online]. Available: https://esc.fsu.edu/documents/CSP/Krothapalli%20Article.pdf

[7] D. Barlev, R. Vidu and P. Stroeve, "Innovation in concentrated solar power," *Solar Energy Materials and Solar Cells*, vol. 95, no. 10, pp 2703-2725, October 2011.

[8] A. Ummadisingu and M.S. Soni, "Concentrating solar power – Technology, potential and policy in India," *Renewable and Sustainable Energy Reviews*, vol. 15, no. 9, pp 5169-5175, December 2011.

[9] S. A. Kalogirou, "Solar thermal collectors and applications," *Progress in Energy and Combustion Science*, vol. 30, no. 3, pp 231-295, 2004.

[10] J.D. Nixon, P.K. Dey and P.A. Davies, "Which is the best solar thermal collection technology for electricity generation in north- west India? Evaluation of options using the analytical hierarchy process," *Energy*, vol. 35, no. 12, pp 5230-5240, December 2010.

[11] P. Heller et al., "Test and evaluation of solar powered gas turbine system," *Solar Energy*, vol. 80, no. 10, pp 1225 – 1230, October 2006.

[12] G. Morin, J. Dersch, W. Platzer, M. Eck and A. Haberle, "Comparison of Linear Fresnel and Parabolic Trough Collector power plants," *Solar Energy*, vol. 86, no. 1, pp 1-12, January 2012.

[13] J. Schlaich, R. Bergermann, W. Schiel and G. Weinrebe, "Design of commercial solar updraft tower systems – Utilization of solar induced convective flows for power generation," *Journal of Solar Energy Engineering*, vol. 127, no. 1, pp. 117-124, February 2005.

[14] V. Quaschning, "Technical and economical system comparison of photovoltaic and concentrating solar thermal power systems depending on annual global irradiation," *Solar Energy*, vol. 77, no. 2, pp 171-178, 2004.

[15] L. Heller. (2013, May). Literature review on heat transfer fluids and thermal energy storage systems in CSP plants. STERG report. [Online]. Available: https://sterg.sun.ac.za/wp-content/uploads/2011/08/HTF_TESmed_Review_2013_05_311.pdf

[16] SAM help. [Online]. Available: https://sam.nrel.gov/download

[17] IRENA. (2018). Renewable power generation costs in 2017. International Renewable Energy Agency. [Online]. Available: https://www.irena.org/-/media/Files/IRENA/.../IRENA_2017_Power_Costs_2018.pdf

[18] IEA-ETSAP and IRENA. (2013, Jan.). Concentrating solar power: Technology brief. [Online]. Available: https://www.irena.org/publications/2013/Jan/IRENA-IEA-ETSAP-Technology-Briefs

[19] IRENA. (2012, June). Concentrating solar power - Renewable energy technologies: cost analysis series, International Renewable Energy Agency. [Online]. Available: https://www.irena.org/documentdownloads/.../re_technologies_cost_analysis-csp.pdf

[20] C. K. Ho. (2008, Dec.). Software and codes for analysis of concentrating solar power technologies. SANIDA report, SAND 2008-8053. [Online]. Available: https://prod.sandia.gov/techlib-noauth/access-control.cgi/2008/088053.pdf

[21] A. Dobos, T. Neises, M. Wagner, "Advances in CSP simulation technology in the System Advisor Model," *Energy Procedia*, vol. 49, pp 2482 – 2489, 2014.

[22] N. Blair, A. P. Dobos, J. Freeeman, T. Neises and M. Wagner, "System Advisor Model, SAM 2014.1.14: General Description," National Renewable Energy Laboratory, Tech. Rep. NREL/TP-6A20-61019, February 2014.

[23] D. Renne, R. George, B. Marion, D. Heimiller and C. Heimiller, "Solar Resource Assesment for Sri Lanka and Maldives," National Renewable Energy Laboratory, Tech. Rep. NREL/TP-710-34645, August 2003.

[24] C. Schillings, R. Meyer and F. Trieb, "High Resolution Solar Radiation Assessment for Sri Lanka," Solar and Wind Energy Resource Assessment, October 2004.

[25] http://solargis.infohttps://encrypted-tbn0.gstatic.com/images

[26] J. A. Duffie and W. A. Beckman, "Concentrating Collectors" in *Solar Engineering of Thermal Processes,* 4th ed., John Wiley and Sons, Inc., pp. 323-325

[27] A. Rabl, "Comparison of solar concentrators", *Solar Energy,* vol. 18, no. 2, pp. 93 -111, 1976.

[28] W. Short, D. J. Packey and T. Holt, "A Manual for the Economic Evaluation of Energy Efficiency and Renewable Energy Technologies," National Renewable Energy Laboratory, Tech. Rep. NREL/TP-462-5173, March 1995.

[29] C. Breyer et al. Assessment of Mid-Term Growth Assumptions and Learning Rates for Comparative Studies of CSP and Hybrid PV-Battery Power Plants. presented at Solar Paces 2016. [Online]. Available: https://aip.scitation.org /toc/apc/1850/1

[30] DNI Cast, Deliverable 5.5, Direct Normal Irradiance Nowcasting methods for optimized operation of concentrating solar technologies, Online. [Available]: http://www.sidosoft.com/dnicast/www/documents/D5.5%20Report%20of%20best%20practice%20guideline%20for%20DNI%20nowcasting.pdf

[31] R. Fu, D. Feldman, R. Margolis, M. Woodhouse and K. Ardani, U.S. Solar Photovoltaic System Cost Benchmark: Q1 2017, National Renewable Energy Laboratory.

[32] D. Kearney et al. (2002, April). Assessment of a molten salt heat transfer fluid in a parabolic trough solar field. Online. [Available]: http://pointfocus.com/images/pdfs/saltw-troughs.pdf

[33] D. Mills, "Advances in solar thermal electricity technology," *Solar Energy*, vol. 76, no. 1-3, pp. 19-31, January – March 2004.

[34] J.I. Ortega, J.I. Burgaleta and F.M. Tellez, "Central receiver system solar power plant using molten salt as heat transfer fluid," *Journal of Solar Energy Engineering*, vol. 130, no. 2, May 2008.

[35] M.J. Montes, A. Abanades and J.M. Martinez-Val, "Performance of a direct steam generation of solar thermal power plant for electricity production as a function of the solar multiple," *Solar Energy*, vol. 83, no. 5, pp. 679 – 689, May 2009.

[36] S. Beerbaum and G. Weinrebe, "Solar thermal power generation in India – a techno-economic analysis," *Renewable Energy*, vol. 21, no. 2, pp. 153-174, October 2000.

[37] E. Hu, Y.P. Yang, A. Nishimura, F. Yilmaz and A. Kouzani, "Solar thermal aided power generation," *Applied Energy*, vol. 87, no. 9, pp. 2881-2885, September 2010.

[38] D. M. Blake et al., "New heat transfer fluids for parabolic trough solar thermal electric plants," in *Proceedings of the 11th SolarPACES International Symposium on Concentrating Solar Power and Chemical Energy Technologies*, September 4-6, 2002, Zurich, Switzerland.

[39] A.S. Withanaarchchi, L.D.J.F. Nanayakkara and C. Pushpakumara, "The progress of Sri Lanka's renewable energy sector developments in mitigating the GHG emission," *Energy and Environmental Engineering 2*, pp. 113-119, January 2014.

[40] Concentrator Optics. Chapter 8. [Online]. Available: http://www.powerfromthesun.net/Book/chapter08/chapter08.html

Appendix A: Location and Resource page (SAM)

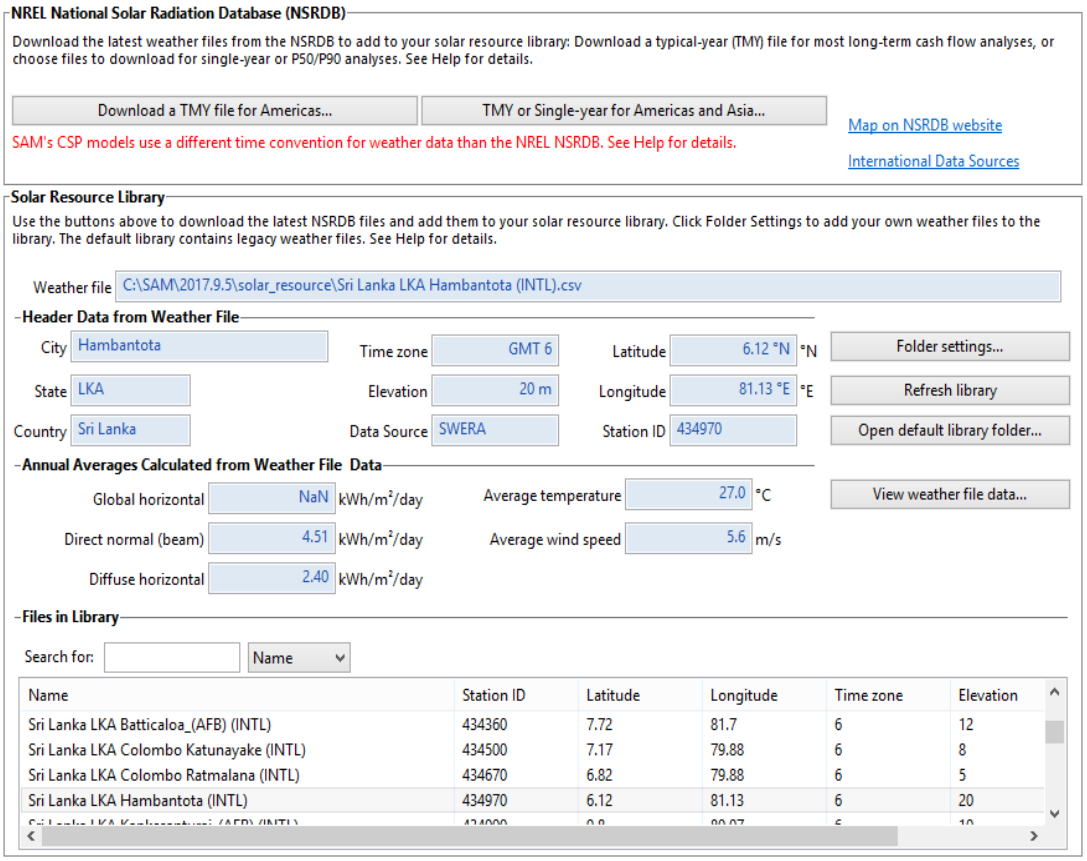

Appendix B: Solar field page (SAM)

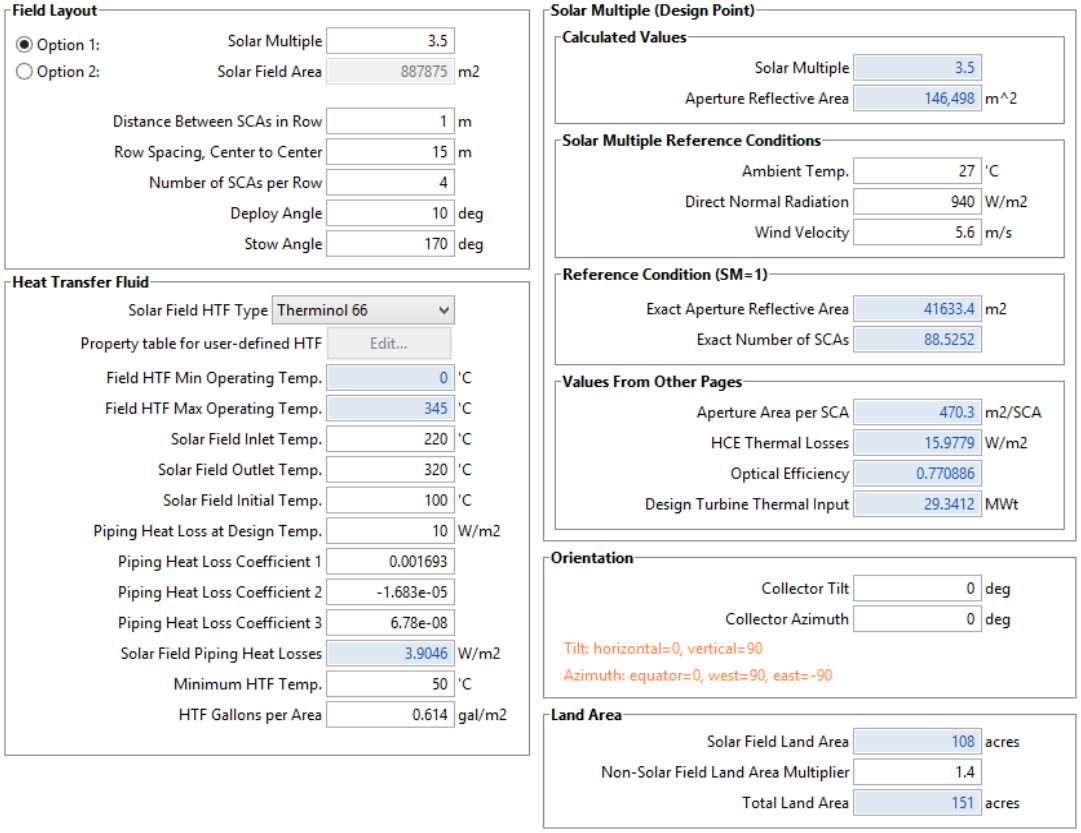

Appendix C: Solar Collector Assembly page (SAM)

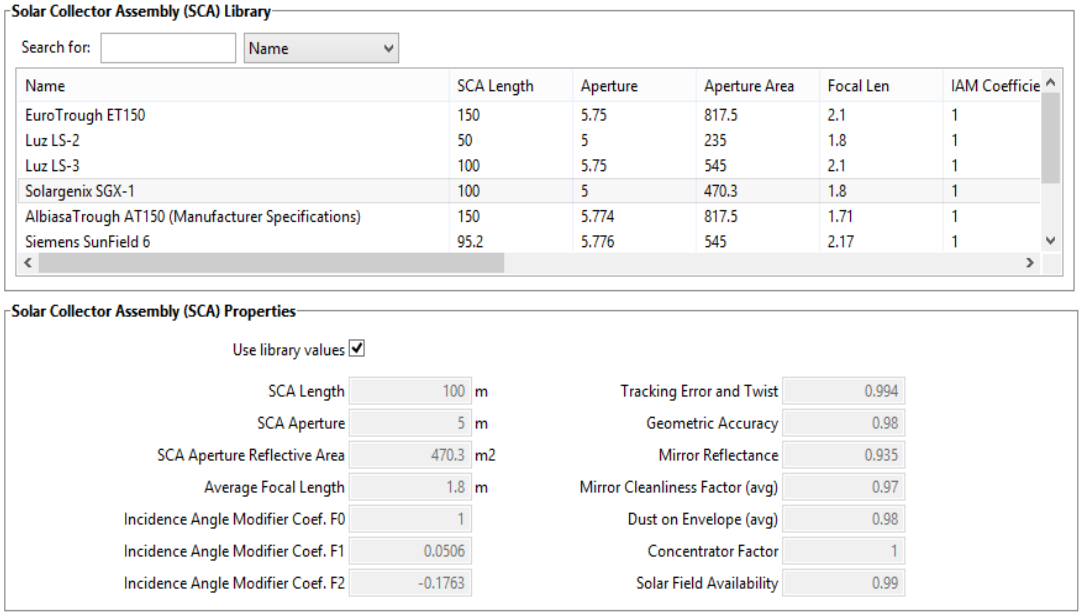

Appendix D: Heat Collection Element page (SAM)

Heat Collection Element (HCE) / Receiver Library

Search for: Name

Name	Broken	Bellows	Transmissivity	Absorption	Unaccounted
Luz Cermet/Fluorescent	0	0.971	0.7	0.8	1
Solel UVAC2 Vacuum	0	0.971	0.96	0.96	1
Solel UVAC2 Lost Vacuum	0	0.971	0.96	0.96	1
Solel UVAC2 Broken Glass	1	0.971	1	0.9	1
Solel UVAC2 Hydrogen	0	0.971	0.96	0.96	1
Solel UVAC3 Vacuum	0	0.971	0.96	0.96	1
Solel UVAC3 Lost Vacuum	0	0.971	0.96	0.96	1
Solel UVAC3 Broken Glass	1	0.971	1	0.9	1
Solel UVAC3 Hydrogen	0	0.971	0.96	0.96	1
2008 Schott PTR70 Vacuum	0	0.963	0.963	0.96	1

Heat Collection Element (HCE) / Receiver Properties

	Receiver 1	Receiver 2	Receiver 3	Receiver 4
	Apply Library	Apply Library	Apply Library	Apply Library
Name from Library	2008 Schott PTR7	2008 Schott PTR7	2008 Schott PTR7	2008 Schott PTR7
Condition from Library	Vacuum	Vacuum	Vacuum	Vacuum
	☐ Broken Glass	☑ Broken Glass	☐ Broken Glass	☐ Broken Glass
Percent of Solar Field:	0.995	0.005	0	0
Optical Parameters:				
Bellows Shadowing	0.963	0.963	0.963	0.963
Envelope Transmissivity	0.963	0.963	0.963	0.963
Absorber Absorption	0.96	0.96	0.96	0.96
Unaccounted	1	1	1	1
Optical Efficiency (HCE)	0.770807	0.786538	0.770807	0.770807
Optical Efficiency (Weighted)	0.770886			

Optical Parameters:				
Bellows Shadowing	0.963	0.963	0.963	0.963
Envelope Transmissivity	0.963	0.963	0.963	0.963
Absorber Absorption	0.96	0.96	0.96	0.96
Unaccounted	1	1	1	1
Optical Efficiency (HCE)	0.770807	0.786538	0.770807	0.770807
Optical Efficiency (Weighted)	0.770886			

Heat Loss Parameters:				
Heat Loss Coeff A0	4.05	4.05	4.05	4.05
Heat Loss Coeff A1	0.247	0.247	0.247	0.247
Heat Loss Coeff A2	-0.00146	-0.00146	-0.00146	-0.00146
Heat Loss Coeff A3	5.65e-06	5.65e-06	5.65e-06	5.65e-06
Heat Loss Coeff A4	7.62e-08	7.62e-08	7.62e-08	7.62e-08
Heat Loss Coeff A5	-1.7	-1.7	-1.7	-1.7
Heat Loss Coeff A6	0.0125	0.0125	0.0125	0.0125
Heat Loss Factor	1	1	1	1
HCE Heat Losses (W/m)	79.8895	79.8895	79.8895	79.8895
Thermal Losses (Weighted W/m)	79.8895			
Thermal Losses (Weighted W/m2)	15.9779			

Appendix E: Power Block page (SAM)

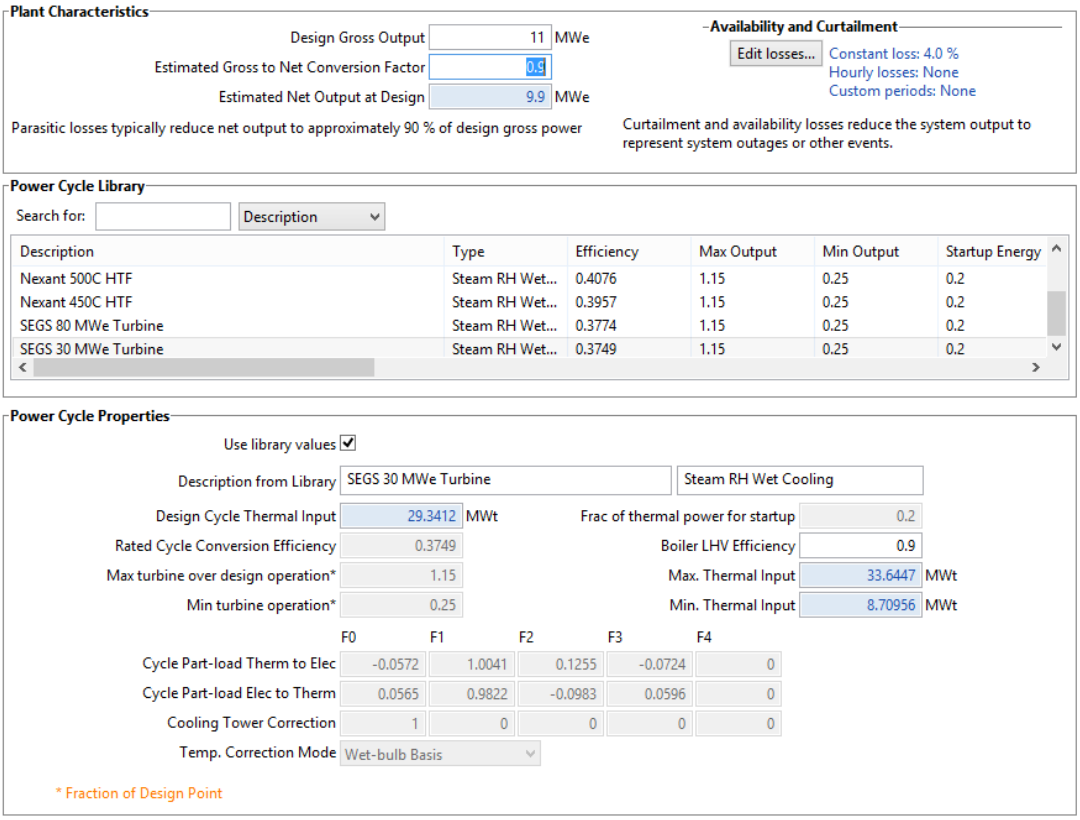

Appendix F: Thermal Energy Storage page (SAM)

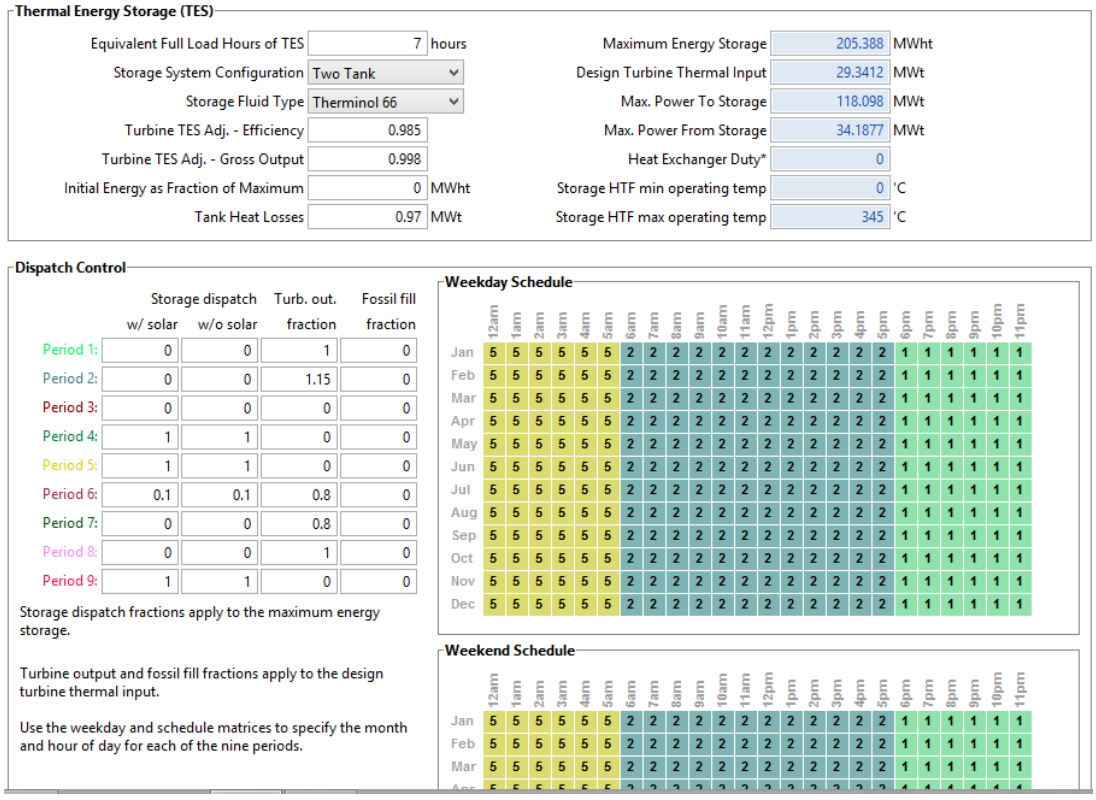

Thermal Energy Storage (TES)

Equivalent Full Load Hours of TES	7	hours	Maximum Energy Storage	205.388	MWht
Storage System Configuration	Two Tank		Design Turbine Thermal Input	29.3412	MWt
Storage Fluid Type	Therminol 66		Max. Power To Storage	118.098	MWt
Turbine TES Adj. - Efficiency	0.985		Max. Power From Storage	34.1877	MWt
Turbine TES Adj. - Gross Output	0.998		Heat Exchanger Duty*	0	
Initial Energy as Fraction of Maximum	0	MWht	Storage HTF min operating temp	0	'C
Tank Heat Losses	0.97	MWt	Storage HTF max operating temp	345	'C

Dispatch Control

	Storage dispatch w/ solar	Storage dispatch w/o solar	Turb. out. fraction	Fossil fill fraction
Period 1:	0	0	1	0
Period 2:	0	0	1.15	0
Period 3:	0	0	0	0
Period 4:	1	1	0	0
Period 5:	1	1	0	0
Period 6:	0.1	0.1	0.8	0
Period 7:	0	0	0.8	0
Period 8:	0	0	1	0
Period 9:	1	1	0	0

Storage dispatch fractions apply to the maximum energy storage.

Turbine output and fossil fill fractions apply to the design turbine thermal input.

Use the weekday and schedule matrices to specify the month and hour of day for each of the nine periods.

Weekday Schedule

	12am	1am	2am	3am	4am	5am	6am	7am	8am	9am	10am	11am	12pm	1pm	2pm	3pm	4pm	5pm	6pm	7pm	8pm	9pm	10pm	11pm
Jan	5	5	5	5	5	5	2	2	2	2	2	2	2	2	2	2	2	2	1	1	1	1	1	1
Feb	5	5	5	5	5	5	2	2	2	2	2	2	2	2	2	2	2	2	1	1	1	1	1	1
Mar	5	5	5	5	5	5	2	2	2	2	2	2	2	2	2	2	2	2	1	1	1	1	1	1
Apr	5	5	5	5	5	5	2	2	2	2	2	2	2	2	2	2	2	2	1	1	1	1	1	1
May	5	5	5	5	5	5	2	2	2	2	2	2	2	2	2	2	2	2	1	1	1	1	1	1
Jun	5	5	5	5	5	5	2	2	2	2	2	2	2	2	2	2	2	2	1	1	1	1	1	1
Jul	5	5	5	5	5	5	2	2	2	2	2	2	2	2	2	2	2	2	1	1	1	1	1	1
Aug	5	5	5	5	5	5	2	2	2	2	2	2	2	2	2	2	2	2	1	1	1	1	1	1
Sep	5	5	5	5	5	5	2	2	2	2	2	2	2	2	2	2	2	2	1	1	1	1	1	1
Oct	5	5	5	5	5	5	2	2	2	2	2	2	2	2	2	2	2	2	1	1	1	1	1	1
Nov	5	5	5	5	5	5	2	2	2	2	2	2	2	2	2	2	2	2	1	1	1	1	1	1
Dec	5	5	5	5	5	5	2	2	2	2	2	2	2	2	2	2	2	2	1	1	1	1	1	1

Weekend Schedule

	12am	1am	2am	3am	4am	5am	6am	7am	8am	9am	10am	11am	12pm	1pm	2pm	3pm	4pm	5pm	6pm	7pm	8pm	9pm	10pm	11pm
Jan	5	5	5	5	5	5	2	2	2	2	2	2	2	2	2	2	2	2	1	1	1	1	1	1
Feb	5	5	5	5	5	5	2	2	2	2	2	2	2	2	2	2	2	2	1	1	1	1	1	1
Mar	5	5	5	5	5	5	2	2	2	2	2	2	2	2	2	2	2	2	1	1	1	1	1	1

Appendix G: System costs page (SAM)

Direct Capital Costs

Site Improvements	146498	m2	26.00 $/m2	$ 3,808,959.75
Solar Field	146498	m2	150.00 $/m2	$ 21,974,768.00
HTF System	146498	m2	60.00 $/m2	$ 8,789,907.00
Storage	205.388	MWht	65.00 $/kWht	$ 13,350,226.00
Fossil Backup	11	MWe, Gross	0.00 $/kWe	$ 0.00
Power Plant	11	MWe, Gross	1,150.00 $/kWe	$ 12,650,000.00
Balance of Plant	0	MWe, Gross	120.00 $/kWe	$ 1,320,000.00
			Contingency 7 %	$ 4,332,570.50
			Total direct cost	$ 66,226,432.00

Indirect Capital Costs

Total Land Area 151 acres Nameplate 10 MWe

	Cost per acre	% of Direct Cost	Cost per Wac	Fixed Cost	Total
EPC and Owner Cost	$ 0.00	11 %	$ 0.00	$ 0.00	$ 7,284,907.50
Total Land Cost	$ 10000.00	0 %	$ 0.00	$ 0.00	$ 1,512,279.63

Sales Tax of 0 % applies to 80 % of Direct Cost $ 0.00

Total indirect cost $ 8,797,187.00

Total Installed Costs

Total Installed Cost excludes any financing costs from the Financing input page.

Total installed cost $ 75,023,616.00

Total estimated installed cost per net capacity ($/kW) $ 7,578.14

Operation and Maintenance Costs

	First year cost		Escalation rate (above inflation)
Fixed annual cost	0	$/yr	0 %
Fixed cost by capacity	66	$/kW-yr	0 %
Variable cost by generation	4	$/MWh	0 %
Fossil fuel cost	0	$/MMBTU	0 %

In Value mode, SAM applies both inflation and escalation to the first year cost to calculate out-year costs. In Schedule mode, neither inflation nor escalation applies. See Help for details.

Appendix H: Financial parameters page (SAM)